Review article

Francesco Poletti*, Marco N. Petrovich and David J. Richardson

Hollow-core photonic bandgap fibers: technology and applications

Abstract: Since the early conceptual and practical demonstrations in the late 1990s, Hollow-Core Photonic Band Gap Fibres (HC-PBGFs) have attracted huge interest by virtue of their promise to deliver a unique range of optical properties that are simply not possible in conventional fibre types. HC-PBGFs have the potential to overcome some of the fundamental limitations of solid fibres promising, for example, reduced transmission loss, lower nonlinearity, higher damage thresholds and lower latency, amongst others. They also provide a unique medium for a range of light: matter interactions of various forms, particularly for gaseous media. In this paper we review the current status of the field, including the latest developments in the understanding of the basic guidance mechanisms in these fibres and the unique properties they can exhibit. We also review the latest advances in terms of fibre fabrication and characterisation, before describing some of the most important applications of the technology, focusing in particular on their use in gas-based fibre optics and in optical communications.

Keywords: microstructured optical fiber; optical communications; gas-based nonlinear optics; optical fiber sensing; laser beam delivery.

*Corresponding author: Francesco Poletti, Optoelectronics Research Centre, University of Southampton, SO17 1BJ, Southampton, UK, e-mail: frap@orc.soton.ac.uk
**Marco N. Petrovich and David J. Richardson:** Optoelectronics Research Centre, University of Southampton, SO17 1BJ, Southampton, UK

1 Introduction

Optical fibre technology plays an ever increasing role in modern society, enabling for example the global internet and communication systems that most of the world now takes for granted, and more recently, providing a new generation of high power laser devices that are finding ever more uses across an increasingly broad range of manufacturing, scientific and medical applications. After more than 50 years of continuous development, and the commercial uptake of the technology, it is perhaps surprising that there is much left to discover and improve when it comes to optical fibres. However, to the contrary, many would contend that we are currently in a golden period for optical fibre research, with several new forms of fibre under development and many intriguing device opportunities emerging. Arguably one of the most exciting of these new fibre types is the Hollow-Core Photonic Band Gap Fibre (HC-PBGF) which, as we shall discuss shortly, guides light in a fundamentally different way to the majority of fibres used around the world today. Critically, this guidance mechanism allows light to be confined over a range of resonant frequencies within a low-index, hollow core which is surrounded by a complex glass microstructure (see Figure 1). This consequently provides for a number of intriguing optical properties including ultralow optical nonlinearity, excellent power handling capabilities, low latency, and even offers the prospect of ultralow losses, both at conventional wavelengths (e.g., around 1550 nm) and at longer wavelengths (i.e., into the mid-IR) at which conventional solid silica fibres effectively cease to transmit light. These properties are unique relative to conventional solid optical fibres and point to a host of exciting application opportunities, both in terms of existing uses of fibre optics (e.g., in telecommunications and the delivery of high power laser light), and new application areas (e.g., gas-based linear/nonlinear optics and lasers, and particle guidance). In this paper we review the current status of the field of HC-PBGFs. We begin with a brief discussion of how such fibres are currently fabricated, before providing a description of the latest developments in the physical understanding of the basic guidance mechanisms and an overview of the key physical properties they exhibit. We focus in particular on the challenges of maximising the useable bandwidth and managing the guided modes in the structure, including those that have useful properties, such as the fundamental and occasionally the first few core-guided modes, and
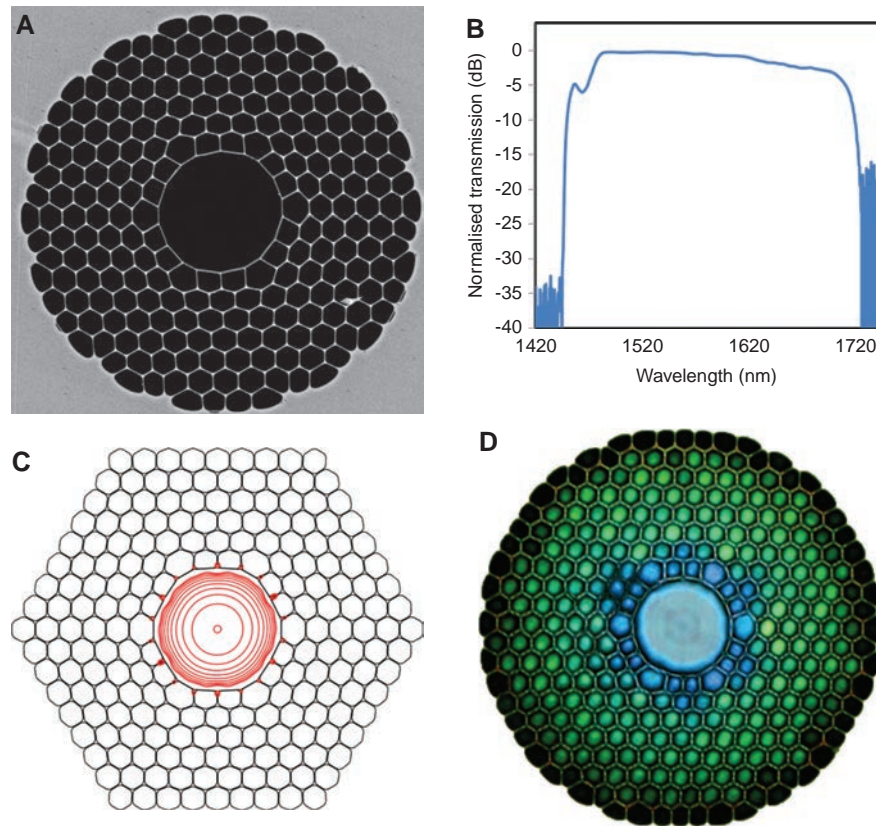
Figure 1 HC-PBGFs guide light predominantly in a central larger air-hole surrounded by multiple periodic holes. (A) is a scanning electron micrograph of a typical fibre, comprising a web of glass membranes as thin as 50–100 nm. The diameter of the microstructured region is typically in the range 80–100 μm, while the core diameter can range from ~5 to 35 μm (see Section 4); (B) shows the typical pass-band transmission spectrum of a 5-m long state-of-the-art near-IR-guiding fibre; (C) is a simulation result showing a contour plot (2 dB spacing) of the intensity profile of the longitudinally propagating fundamental guided mode for a wavelength inside the bandgap: more than 99% of the optical power can be transmitted in air; (D) is an example of a colourful pattern, arising from antiresonances and high order band gaps that can be seen when observing an IR-guiding fibre under an optical microscope.

those that substantially degrade the usefulness of the fibre, i.e., surface modes and higher-order core-guided modes. Finally, we review some of the most important applications of the technology. We begin this last section by describing improvements in splicing and the manufacture of gas cells that have substantially improved the practicality and utility of these fibres, and briefly describe some of their applications in gas-based fibre optics, sensing and lasers. We conclude by describing recent progress in the use of the fibres in optical communications – arguably the most demanding of all application spaces.

2 The basics of HC-PBGF fabrication

As can be seen in Figure 1, a typical HC-PBGF comprises one to two hundred wavelength-scale air holes, normally with a very high air filling factor, arranged in a 2-D array

that is maintained along the full length of the fibre. Given the resonant nature of the guidance mechanism, the complex transverse structure of the fibre, which contains features as small as ~100 nm or less, needs to be preserved with minimum longitudinal structural variation over lengths ranging from several metres up to several kilometres.

Currently all groups worldwide use the stacking technique, which is inspired by techniques developed for the fabrication of microchannel plates [1] and in part derived from older methods utilised to produce solid fibres before the widespread success of chemical vapour deposition methods. In this approach [2, 3], bundles of metre-long, ~mm diameter glass capillaries are manually assembled according to the required geometry and tightly packed inside a jacketing tube to form the primary preform (typical diameter in the range 20–30 mm, see Figure 2A). In the case of triangular, close packed geometries, which are the most natural stacking arrangement for circular
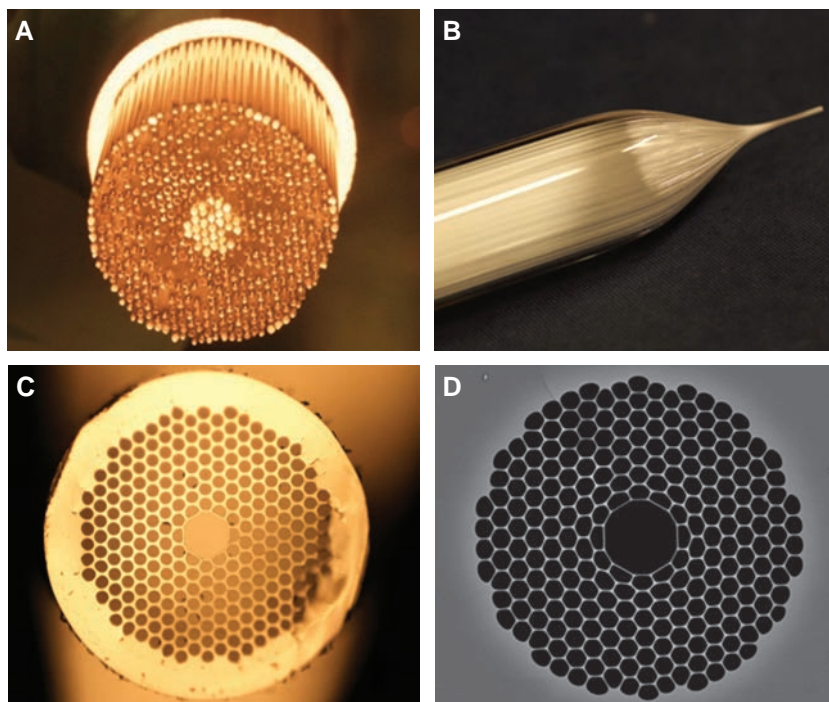
Figure 2 HC-PBGFs fabrication process flow using the "stacking" (or "stack and draw") technique: (A) primary preform obtained by assembling a few hundred high purity, low-hydroxyl silica glass capillaries into an array with the required geometry tightly packed inside a glass tube; (B) first stage draw of the primary preform into a ~millimetre sized "cane"; (C) optical image of the cross-section of a HC-PBGF cane showing elimination of interstitial volumes and formation of the central core "defect"; (D) scanning electron microscope image of the microstructured region of the final fibre, showing a much increased diameter to pitch ratio of the cladding holes. The typical hole-to-hole spacing for operation at 1500 nm wavelength is in the range of 4–6 µm (depending on the air filling ratio of the cladding).

capillaries, simple jigs can be used and gravity exploited to help form and order the target structure. The core can be obtained either through the use of a larger tube placed at the centre of the array, or by removing an appropriate number of capillaries and suitably supporting the stack at its extremities to maintain structural integrity. It is interesting to point out that the very first HC-PBGFs were obtained without the use of a core tube element, which was later introduced when the advantages it presents in controlling structural stability in highly "inflated", high air-filling fraction fibres became apparent. The tube was eliminated once again more recently, when it was recognised that fibres with a thinner core surround can provide a wider effective bandwidth and improved modal qualities (see Section 3.3).

The material of choice is normally synthetic low-hydroxyl "dry" silica glass (e.g., Suprasil F300 from Hereaus or equivalent), although use of other grades of synthetic silica (F100, F320) is also possible and has been explored in some works [4].

While other air/silica microstructured fibre types (for instance those with a solid core and a large mode area) can be achieved from stacked preforms in a single fibre

drawing step, HC-PBGF preforms require an intermediate step (see Figure 2B and C) in which the primary preform is fused and scaled down to a "cane" (typically 1–3 mm diameter). Here high temperature and pressure differentials are utilised in order to form the interconnected lattice of rods in the cladding (e.g., by eliminating undesirable interstitial volumes between capillaries) and to form the core.

In a further step, the cane is placed in a second jacketing tube and the assembly drawn into the final fibre with a typical external diameter of 100–200 µm. In this case, pressure differentials are used to substantially increase the ratio between hole diameter and inter-hole separation (or pitch) d/Λ of the cladding holes, while scaling down their overall size (see Figure 2D). As will be discussed in later sections, a high air filling factor is required to achieve a wide, low loss transmission window. For a given expansion ratio, the cladding pitch is fine tuned to obtain operation at the required wavelength, according to a scaling rule discussed in Section 3.1. It should be noted that the requirement for a two-step fibre draw is mainly dictated by the convenience in having an intermediate step which is useful in order to eliminate interstitials between

capillaries and to achieve a final high air filling fraction of cladding holes while also controlling the core boundary. Having two draw stages with different drawing tensions also helps reduce hole distortions [5]. However it does not appear impossible that a suitable single step procedure could be devised in the future, particularly as the size of the primary preforms is scaled up in order to increase the fibre yield per draw.

The second stage fibre draw is accomplished using a conventional fibre draw tower, however the drawing process is significantly more involved than for conventional fibres. For HC-PBGFs the temperature is generally kept relatively low (by approximately ~50°C) as compared to solid fibres in order to keep the glass viscosity high and oppose hole collapse. Also, for the same reason the drawing tension applied to the fibre is typically 50–100% higher than in standard solid fibres for otherwise equivalent fibre draw parameters Furthermore, the differential pressure inside holes of different sizes effectively becomes an additional critical draw parameter. Since the larger central core hole requires comparatively lower pressure than the cladding holes to achieve the same expansion ratio, means to accurately control the pressure difference in different regions of the cane need to be implemented. Good quality HC-PBGFs were achieved in the past by passively pressurizing the canes in the second stage draw, i.e., by sealing their top face and exploiting self-pressurisation as a self-stabilising mechanism to control pressure variations [6–8]. More recent fibres, however, are typically produced by actively and independently controlling multiple pressure zones within the preform [9, 10] in order to obtain a higher degree of control over the relative expansion of core and cladding holes. Since small differences in the core boundary can have very strong effects on the transmission and modal properties of HC-PBGFs, accurate control of the differential pressure between core and cladding holes (tolerances at the level of ~0.1 kPa) is of paramount importance.

Establishing the required draw conditions needed to realise the desired optical/structural properties is a challenge and requires means to monitor and characterise the structure (and the gross optical properties) of fibre samples taken during the early phase of the draw, as well as considerable experience and skill on the part of the fabricator. To aid in this process various hardware and software tools have been developed. For example we recently reported a simple model based on the principle of mass conservation [11] that allows a prediction of the geometrical parameters of the final fibre (and thus its optical properties such as photonic bandgap position and width) from the structure of the originating canes and simple

parameters easily measurable during the fibre draw (i.e., the fibre outer diameter). Such tools are of immense value in minimising the time spent optimizing the pulling parameters and ultimately help to increase the fibre yield.

Typical second stage preforms can produce up to a few km of stable fibre – for example we are currently able to obtain up to 5 km of usable fibre in a single draw. While a detailed description of methods to increase the draw yield to beyond 10 km have not yet emerged in the literature, this topic is beginning to gain traction as HC-PBGFs are emerging as credible candidates for both long and short haul data transmission applications.

Although the basic "stack-and-draw" process may appear crude (and perhaps more prone to contamination as compared to vapour deposition processes), it has proven both highly flexible and capable of producing high quality HC-PBGFs of various forms in considerable lengths. As the need for larger preform sizes emerges this may open up opportunities to try other approaches to preform manufacture such as sol-gel casting [12], mechanical drilling [13] or laser drilling [14]. Initial attempts have been made using these approaches in simpler microstructured fibres, but never on fibres with as complex a cross section as a HC-PBGF.

3 Optical guidance in photonic bandgap fibres

The unique properties of HC-PBGF largely originate from their ability to propagate light in an air core. In this section we describe the fundamental guidance mechanisms that underpin and impact optical guidance in HC-PBGFs, providing new insight into the origin and impact of surface modes that can compromise the performance of current fibres.

3.1 Photonic bandgap formation and out of plane guidance

HC-PBGFs guide light in a central hollow core by virtue of the presence of a photonic bandgap (PBG) in the periodic surrounding holey dielectric cladding region. The PBG prevents light at well-prescribed wavelengths and angles of incidence from propagating into the cladding and hence allows tight optical confinement in a suitably designed low refractive index central defect.

In analogy with the electronic bandgaps of solid-state physics, which arise from a periodic arrangement of

atomic potentials that generate forbidden energy bands for the electrons, photonic bandgaps originate from the periodic arrangement of two different dielectrics and which gives rise to a frequency band of forbidden propagation for photons confined and guided in the structure [15, 16].

The necessary condition for the creation of PBGs suitable for guidance in a low refractive index material is that the ratio between the wavevector components in the plane of periodicity for the two dielectrics, k_{p1}/k_{p2}, must exceed a certain critical value which depends on the specific lattice arrangement under consideration. In practice, for light propagating *in the plane of periodicity*, a large refractive index difference between the two dielectrics is needed, e.g., Δn>2.2 for a triangular arrangement of circular holes [17], which substantially limits the possible choice of dielectric pairs and leaves only high refractive index glasses or semiconductors as viable material choices for air-guidance. Back in the early 1990s though, Russell had the insight that should the periodic dielectric arrangement be infinitely elongated in the third dimension, for light propagating *out-of-plane*, it should be possible to achieve any desired k_{p1}/k_{p2} ratio – and therefore to open up a PBG for *any choice* of dielectric pairs [17]. The trick here lies in choosing the direction of propagation at a sufficiently small angle with respect to the normal to the plane of periodicity [18, 19]. This initial conceptual breakthrough, followed by a few years of intense technological effort to develop the required fibre fabrication technology, led to the first demonstration of a HC-PBGF made of a "holey" glass structure, which guided light in air (albeit with relatively high losses in the first instance) despite the comparatively modest refractive index difference of only 0.44 between the chosen glass (silica) and air [3].

Early numerical studies of PBG guidance in hollow core silica fibres focused on identifying the best lattice and core defect arrangement to generate wide band gaps in structures able to support air-guided modes [20–22]. These studies were based on numerical techniques adapted from solid-state physics for the calculation of the frequency bands of a unit cell with periodic Bloch boundary conditions as a function of wavevector direction [15, 23, 24]. While providing a very useful steerage in the early fibre designs (e.g., the conclusion that a triangular lattice of holes would support a stronger air-guidance than a honeycomb lattice [21], or that the bandwidth scales to a first approximation with the air-filling fraction of the fibre [22]), these methods were limited to the analysis of perfectly symmetric and infinitely extended lattices and therefore did not permit the study of the defect modes within the fibre. A number of alternative methods have therefore subsequently been newly derived, or adapted from existing approaches, to allow the study of realistic fibre structures incorporating core defects and periodic claddings of finite extent. These second-generation studies were based on, for example, plane-wave expansion [25], finite element [26], multipole [27] or finite difference methods [28]. The downside of all these brute-force numerical techniques is that they fail to capture and explain the physical mechanisms generating the PBG and do not provide any insight into how structural perturbations of the cladding periodicity and/or distortions at the defect termination affect the optical properties of the fibre. More recently, simple models originating from a fibre optic rather than a solid-state physics perspective have been put forward to explain PBG formation and guidance as a result of anti-resonant interactions in arrays of closely spaced resonators (also referred to as rods or apexes) in the fibre cladding [9, 29].
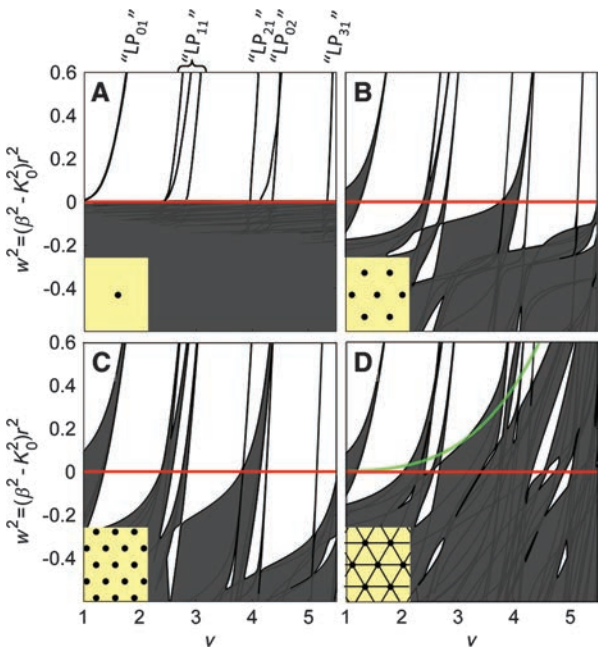
Figure 3 illustrates the origin of air-guiding band gaps in HC-PBGFs using such concepts. Figure 3A shows the well-known dispersion relations for a simple circular silica glass rod in air. The different curves indicate the dispersion of the various modes guided in the rod as a function of its *v* parameter ($v=2\pi r\sqrt{n^2-1}/\lambda$, where *n* is the glass index, *r* the rod radius and λ the wavelength of operation). Below the air-line, indicated in these plots by $w^2=(\beta^2-k_0^2)r^2=0$, where β is the longitudinal propagation constant and $k_0=2\pi/\lambda$ the wavenumber in air, a continuum of plane-wave-like air modes exists (grey area). Above the air line, indicated in white, there are regions in the (v, β) plane where no modes can propagate in the cladding, nor can they be sustained in the rods, i.e., they are in *antiresonance* with them. By bringing a number of identical rods sufficiently close together the dispersion relations can be substantially modified (Figure 3B). Notably, the dispersion curve of each mode close to its cut-off condition ($w^2\sim0$ or $\beta\sim k_0$) broadens as a continuum of allowed guided states. In practice, at sufficiently low values of *v*-number, the modes of a single rod become so expanded into the cladding that they start to significantly overlap with neighbouring rods. The coherent spatial superposition of modes from individual rods forms a band of supermodes with its own range of allowed effective indices, in close analogy to the energy splitting of closely spaced atoms (tight binding model) [9]. Most importantly, a *periodic* sequence of multiple forbidden guidance regions (e.g., PBGs, shown in white in Figure 3B) opens up for some values of (v, β) below the air-line. If a suitable defect, able to support modes in this PBG region, is created in the cladding, for example by omitting one or more rods, light can be confined therein. As the rod separation decreases (Figure 3C), the interaction between rod-guided modes becomes stronger and it ultimately widens the supermode bands, with the result of narrowing the frequency width of the air

band gaps. Also, the low refractive index area in between rods is reduced, which has the effect of making the PBGs deeper and hence able to support a larger number of air-guided modes for the same defect size. Note that a similar guidance mechanism occurs in all-solid PBG fibres formed by an array of up-doped rods (with typical Δn~1–3%) surrounding a low-index defect [29], with the difference that for air-guiding HC-PBGFs the relatively high index contrast between silica and air makes vector effects more prominent. These cause, for example, the evident splitting between the dispersion curves of vector modes belonging to the same "LP" group (see Figure 3A).

A second, even more fundamental difference is that rods in a realistic air cladding need to be physically interconnected. Figure 3D shows what happens when a thin network of interconnecting struts (also silica glass) are added to the structure. As can be seen, the periodic band gap structure is profoundly modified, with high order

Figure 3 Creation of an air-guiding photonic-band gap: (A) shows the dispersion of the (vector) modes guided in a circular glass rod of dimensions comparable to the wavelength and surrounded by air (see structure in the inset). In the grey area a continuum of air-guided modes exists, while in the white regions no guided states are supported in either the rod or the cladding; (B) shows that, by bringing several identical rods sufficiently close together, multiple band gaps extending below the air line (here indicated in red), can be formed; in (C) the air-guiding bandgaps become deeper and narrower as the inter-rod distance is reduced; (D) shows the effect of struts interconnecting the cladding rods as disposed in a realistic fibre structure: the high-order band gaps become distorted and only the lowest frequency one remains below the air-line and can hence support an air-guided mode. This typically occurs for v-numbers in the range 1–2.

bandgaps being shifted to higher effective indices and ultimately above the air-line. This can be explained by the fact that, unlike the dispersionless air cladding, the effective index of the cladding formed by such thin struts has a strong wavelength dependence. At high v numbers light becomes more confined in the glass struts, thus raising the effective index of this structured cladding (or more precisely of its fundamental space filling mode, the dispersion of which is shown by the green line in Figure 3D). The PBGs of higher orders (at larger v) are the most affected and tend to shift above the air-line even for the thinnest struts that are realistically achievable. The final result is that, differently from the multiple PBGs observed in all-solid band gap fibres [29], HC-PBGFs typically only support a single PBG, and hence they only guide over a range of frequencies that is normally contained in the interval $1 \leq v \leq 2$. This is the scaling law for a HC-PBGF [19], and it indicates that in order to shift the operational wavelength range, it is sufficient to scale the resonator size so that r/λ remains constant. In practice this result can be more easily achieved through a simple rigid scaling of the entire microstructure.

Note that although the example in Figure 3 refers to a periodic triangular arrangement of circular rods, the qualitative conclusions drawn here are also valid for other lattices and for structures with non-circular (e.g., triangular-like) rods. Furthermore, it is clear that it is the rod size that is primarily responsible for the PBG creation. As long as the rod sizes are kept constant, small variations from their optimum position in the lattice will have a very small effect on the HC-PBGF band gap properties, as is frequently seen in the fabrication of HC-PBGFs incorporating large core defects (e.g., with 19 omitted cells or bigger), which often exhibit claddings that are compressed or expanded in the radial direction and have an irregular distribution of rods within the core surround.

3.2 PBG bandwidth

Since HC-PBGFs can only guide at frequencies where the PBG exists, considerable effort has been devoted since the early days to understand the influence that a particular choice of lattice arrangement, air hole shape or size, and glass refractive index have on the resulting width of the band gap, with the general goal being to obtain as broad a usable bandwidth as possible. A general finding in all the initial numerical studies was that band gaps becomes larger as the air-filling fraction of the cladding increases, with other details of the unit cell playing a role but being of lesser impact [22, 26]. This can be explained by recognizing that a higher fraction of air in the periodic unit

cell leads to thinner interconnecting struts. Since, as we have seen, these structural features distort all band gaps and thus negatively affect the guiding properties of the HC-PBGF, reducing the strut thickness generally leads to a less distorted and hence a broader fundamental bandgap.

While, as discussed, most of the HC-PBGFs fabricated to date have a cladding formed by a triangular lattice of holes (TLH) (see Section 2), other lattices have been studied and some of them have been found capable of generating even wider band gaps. For example, for the same ratio of strut thickness to inter-hole (pitch) distance t/Λ, which is one of the most critical parameters that needs to be minimised during fibre fabrication, HC-PBGFs with holes arranged in a square lattice (SL) can provide a ~20% wider PBG width than TLH lattices [30]. An even wider band gap can be achieved in a fibre where the rods rather than the holes are arranged on a triangular lattice (i.e., in a triangular lattice of rods or TLR) and the holes are thus forced to assume a triangular shape [31] (see Figure 3D, inset). For the same t/Λ, this lattice generates thinner struts than the TLH and SL and as a result it can support considerably wider band gaps, which can theoretically span up to an octave (i.e., covering the spectral range from ω to 2ω) for very high (but attainable) values of air-filling fractions [32].

Whilst achieving a TLR lattice and related core defect is complicated using standard fabrication methods, and this has prevented so far the practical demonstration of a TLR fibre, an ultra-wide bandwidth HC-PBGF based on the SL has been demonstrated [33]. Owing to an extremely high air filling fraction which led to strut thicknesses of only a few tens of nanometres, the fibre supported a relative PBG width Δf_r (bandgap width over central frequency) of 44%, currently the widest band gap ever reported for a HC-PBGF. For comparison, commercially available TLH-based fibres typically have Δf_r around 10–15%, while the broadest reported TLH has a bandgap width of around 33% [34].

Whist achieving a broad bandwidth is critical for many applications, e.g., nonlinear optics or data transmission, it is less of an issue in others, e.g., high power laser delivery, where the laser wavelength is generally well specified and narrowband; in the latter case, bandwidth can be traded off to provide greater flexibility in manufacture, or improved performance in terms of other optical properties (e.g., dispersion). In general though, having access to more rather than less bandwidth is beneficial.

It is finally worth mentioning that a number of works have studied the dependence of the out-of-plane bandgap guidance on the refractive index of the glass. While it is theoretically possible to achieve HC-PBGFs from glasses with a higher refractive index (and transmitting at longer wavelengths) than silica, due to the increasing importance

of vector effects, the bandgaps are generally found to be narrower [35, 36]. Interestingly, they are obtained by claddings at significantly lower air-filling fractions than those required in silica HC-PBGFs. Some promising experimental work in this direction has been attempted with a chalcogenide glass (n~2.9) [37].

3.3 Surface modes

The PBG bandwidth available for light guidance in the low index (air) core produced by any particular periodic cladding only provides an upper theoretical limit to the useable bandwidth available in the HC-PBGF. In practice, the creation of a light-guiding core requires termination of the periodic lattice that creates the bandgap and thus the formation of an artificial boundary. Similar to what happens in solid-state physics at the semiconductor edge, where surface states can be supported at energies within the bandgap, the sudden termination of the periodic dielectric structure in the cladding of HC-PBGF can introduce spurious guided modes, referred to as surface modes (SMs). These are physically localised at the core surround interface and are spectrally guided at wavelengths within the bandgap. If symmetry allows, these generally lossier and more dispersive modes can anti-cross with core-guided modes. When this happens, a supermode forms in the vicinity of the anti-crossing wavelength, and is spatially localised partly in air and partly at the core surround interface. Consequently, it experiences far greater propagation losses than the normal air guided modes [38–40]. This SM anti-crossing generally has several detrimental consequences: besides a reduction in the useable bandwidth and an increase in the propagation loss of the fibre, it also causes an increased sensitivity to external perturbations [41] and undesirable polarisation properties such as a high polarisation dependent loss and strong polarisation mode coupling [42].

For these reasons, a number of studies have been devoted to developing effective measures to eliminate SMs by optimising the core surround/photonic crystal termination. Early works focusing on idealised fibres made of an array of regularly arranged *circular* holes concluded that the size of the core defect was crucial and proposed idealised core terminations for SM-free operation [43–45]. However, in practice, fibres with a high air-filling fraction tend to have hexagonally rather than circularly shaped holes, and the interplay of surface tension and differential pressures during fabrication substantially limits the design space available to eliminate SMs. A useful practical step forward towards the realisation of wide bandwidth, SM-free fibres came from systematic numerical studies of

more realistically achievable structures, with hexagonally shaped cladding holes and typical core shapes [46, 47]. These studies showed that a critical parameter for the control of SMs was the core surround thickness T. In particular, simulations revealed that if S is the average thickness of the struts in the cladding, for $T\sim S/2$ realistic fibres with no SMs across the full bandgap can be realised.

Despite its usefulness in providing practical guidance on how to realise SM-free wide bandwidth fibres, this empirical rule, derived by a numerical brute force approach, fails to provide physical insight on the origin of SMs. Moreover, it is restricted to rather ideal cases where the cladding periodicity is well maintained and no distortions are present in the core surround, which is typically not the case for the larger core HC-PBGFs of interest for ultra-low loss operation (see Section 4).

It is possible to gain a deeper physical insight on the origin of SMs by returning once more to the interconnected antiresonant rod picture that we have already invoked to explain PBG guidance [48]. Figure 4 shows the bandgap-map ($n_{eff}=\beta/k_0$ vs. wavelength) for a periodic cladding formed of silica rods interconnected by thin silica struts as in a TLH lattice; the element size is chosen to resemble that of a typical HC-PBGF guiding in the near infrared, with rod diameter and strut thickness of 600 and 120 nm, respectively. The area below $n_{eff}=1$ indicates the PBG region available for air guidance. The bandgap is bound by three different types of cladding modes: at short wavelengths by a mode mostly localised in the struts, at long wavelengths by a mode mostly localised in the rods, while its lower n_{eff} edge is formed by air-localised modes [49]. Terminations of the periodic cladding to form the core defect may perturb this situation and induce a set of modes strongly localised at the boundary (i.e., SMs) that are guided inside the bandgap. For example, if the termination introduces struts that guide modes of a higher effective index than in the uniform periodic cladding (e.g., if the struts are longer or thicker), a strut-localised SM (*sSM*) will enter the PBG region from the short wavelength edge. Likewise, if the termination comprises rods with a lower effective index than the average in the cladding (e.g., if the core surrounding rods are smaller or more closely spaced), a rod-localised SM (*rSM*) will enter the PBG from the long wavelength edge. Two typical examples are shown in Figure 4. Interestingly, a well-known example of sSM, probably the most frequently observed SM in HC-PBGFs, is that supported by the pentagonal holes surrounding the core. Any conceivable realistic core shape obtained by stacking circular capillaries in the preform always results in some of the core surrounding holes having only five rather than six nodes and sides, with the side sitting on the core boundary longer than the others.

Therefore, if the core surround thickness is equal or greater than that of the average cladding struts, this longer core surround segment will end up supporting one or more SMs. This occurs in several fibres of historical relevance [50, 51]. With this physical interpretation in mind it is now easy to understand the $T\sim S/2$ rule: by thinning the core surround, the effective index of the SMs can be reduced sufficiently to shift them back outside of the bandgap [47].

Producing fibres with $T\sim S/2$ requires stacks where the defect is simply created by omitted capillaries, with no additional core tube. Although the absence of a supporting core tube introduces some additional fabrication complexity, effectively reduces the yield of first stage draws and makes the fabrication of reproducible fibres more challenging, fibres with "reduced" core thickness have nonetheless been fabricated. Experimentally they were shown to provide efficient suppression of surface modes, leading to very wide transmission bandwidths [6, 7].
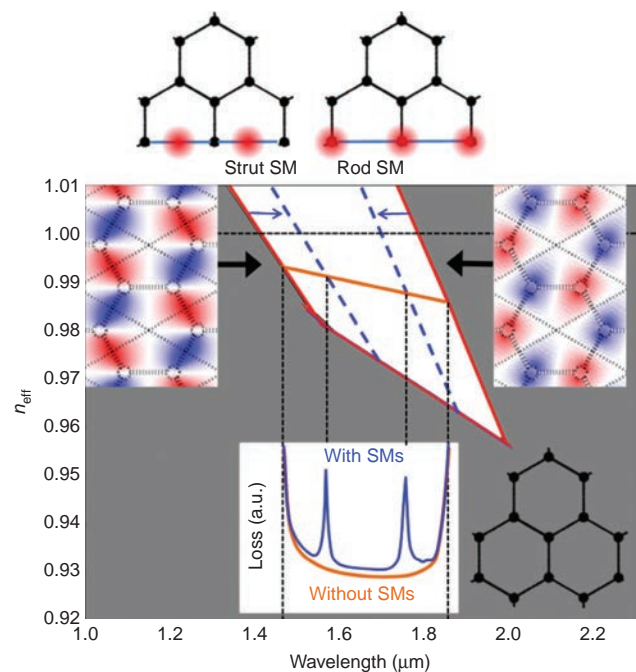
Figure 4 Origin of surface modes. The white area indicates the photonic bandgap of a typical HC-PBGF cladding, formed by a periodic arrangement of rods interconnected by thin membranes (shown in black in the bottom right corner). The strut-localised and rod-localised modes forming the short and long wavelength edge, respectively, are also shown. When a core defect is created, as a result of structural perturbations, some of these modes can be brought inside the bandgap, forming either a strut-localised or a rod-localised surface mode. Surface modes (blue dashed lines) can anti-cross with air-guided modes (orange solid line) and generate spectrally localised regions of high loss which reduce the HC-PBGF bandwidth and adversely affect the fibre performance (see main text).

Building on these results, a 7c HC-PBGF combining the lowest loss reported to date for this type of fibre (9.5 dB/km at 1650 nm) and a wide transmission BW (~140 nm) was later demonstrated [52] (Figure 5D). Further studies have also shown that close to SM-free operation can be achieved even if the core surround is slightly thicker than *T=S/2*, which is compatible with the use of an extremely thin core tube [54]. More recently, the thin surround concept has also been applied in fibres with larger core defects formed by 19 and 37 missing capillaries [10, 55]. While very wide bandwidths were achieved in these cases, unavoidable distortions in the region of the core surround due to the fact that surface tension favours the creation of a circular defect from the initial hexagonal core shape prevented the complete elimination of SMs from within the PBG. Further studies on fibre structures with such large core defects incorporating a more realistic circular core surround arising from the action of surface tension during fibre drawing have shown that one possible way to circumvent this limitation is to target the fabrication of fibres with equally spaced nodes on the core surround [48]. In this case the fibre would not support

SMs even in the presence of a thicker core surround introduced by a core tube, which offers several potential practical advantages.

4 Controlling loss and modality in HC-PBGFs

In this section we review the prospects and issues with regards to simultaneously achieving low loss, and broad bandwidth whilst enabling effectively single mode or controlled multi-mode guidance, as desired by a specific application. Trade-offs are inevitably required and the options are further constrained by features of the fabrication process itself.

4.1 Propagation loss in HC-PBGFs

As for every fibre technology, propagation loss plays a crucial role in determining the range of applications that a
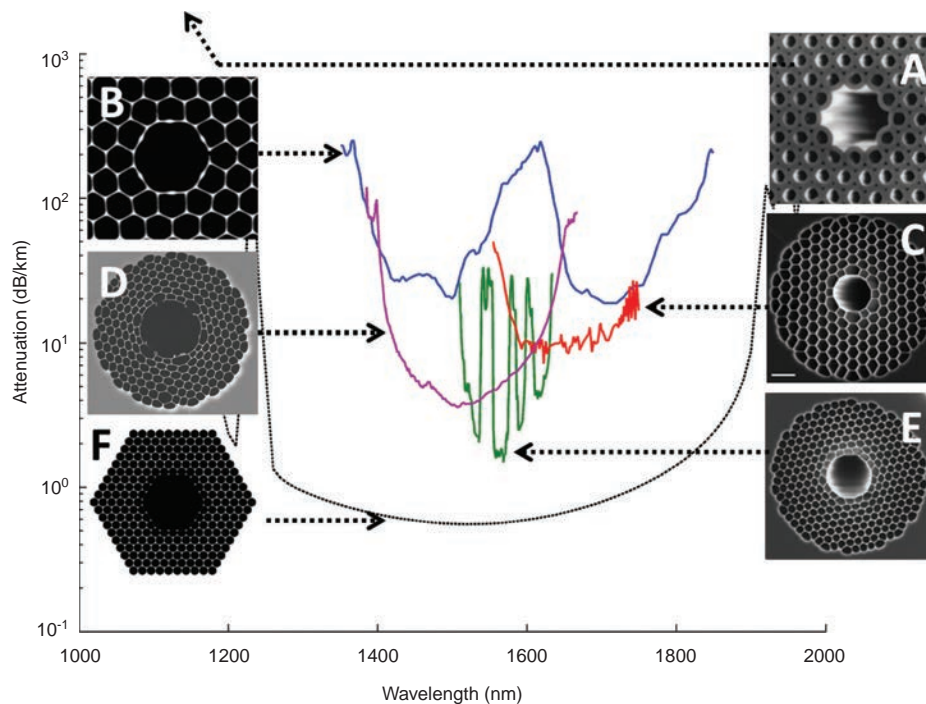
Figure 5 Milestones in HC-PBGF development from early demonstrations to the most recent fibres: (A) the first fibre demonstration had a relatively low air filling factor leading to high losses (>100 dB/m at visible wavelengths for [3] and ~1 dB/m at 1300 nm for [53]); (B) first example of HC-PBGF with a high cladding air filling factor, achieving a loss of 13 dB/km [50]; (C) first surface mode-free HC-PBGF with a 7 cell geometry and a loss of 9.5 dB/km (lowest reported loss for this core size) [52]; (D) 19 cell HC-PBGF recently fabricated by the University of Southampton showing a record combination of low loss (3.5 dB/km) and wide bandwidth (~160 nm) [10]; (E) record low loss HC-PBGF obtained through the use of a thick, anti-resonant core surround [51]: the lowest properly documented loss of 1.7 dB/km was achieved at the expense of the useable bandwidth, limited to ~20 nm; (F) simulated total loss (scattering and confinement) for an optimised 37c fibre operating at 1550 nm showing what might ultimately be possible through further refinement of the fabrication process.

fibre can be used for. Nowhere is loss more critical than in the case of optical communications – long-haul data communications in particular for obvious reasons. Conventional all-solid fibre technology has matured and benefited from more than three decades of technological improvements and massive financial investment, and it is now close to fundamental and insurmountable physical loss limits imposed by Rayleigh scattering. Initial work on hollow fibres was indeed prompted by the consideration that the Rayleigh scattering loss of dry air is only $7 \cdot 10^{-4}$ dB/km, more than 200 times lower than in pure silica glass, raising the question as to whether HC-PBGFs could ever surpass conventional all-glass fibres and become the ultimate ultra-low loss optical waveguide.

Figure 5 shows the cross-section and loss of some of the most important and representative HC-PBGFs reported to date. The first demonstration of hollow core guidance was achieved in 1999 by the group at the University of Bath [3] (see Figure 5A). In the early days of HC-PBGF development, efforts were predominantly aimed at achieving microstructure with sufficiently high regularity to support bandgap guidance, however the low air filling factor achieved only allowed losses at the ~dB/cm level. Subsequent activity concentrated more closely on the improvement of fibre properties, and fibres with loss around ~1 dB/m were soon after reported [53]. A substantial breakthrough (Figure 5B) was obtained by the specialty fibre division of Corning who successfully pushed the air filling fraction from <50% to beyond 90%, resulting in a two orders of magnitude reduction in transmission loss (13 dB/km at 1500 nm) [50]. Through a further increase in air filling fraction the loss in a 7c HC-PBGF was recently further reduced to 9.5 dB/km [52] (Figure 5C).

In parallel, evidence begun to emerge that a different form of light scattering from the mechanism that limits loss in solid fibres (i.e., Rayleigh scattering) played a dominant role in HC-PBGF scattering from residual roughness at the air-glass surfaces [56]. While other loss contributions such as the confinement or leakage loss can be managed simply by making the radial extent of the photonic crystal cladding sufficiently large (i.e., by introducing a sufficient number of rings of air holes), reducing surface scattering loss has proved to be more challenging. Although the electromagnetic field intensity at the core surround interface is already 2–3 orders of magnitude lower than in the central part of the core and despite the fact that glass surfaces in a fibre can be made smooth to nearly atomic levels (with measured *rms* values of only ~0.2 nm over the spatial frequencies that can be measured using atomic force microscopy), the index contrast between air and glass is sufficiently high to cause dB/km loss levels in current state-of-the-art HC-PBGFs [57].

To reduce surface scattering effectively, researchers at the University of Bath have worked to reduce the amount of field overlap with the air/silica interface at the boundary of the core and of the air holes located in its close proximity by designing fibre incorporating "antiresonant" core boundaries. Here the core surround thickness is made to be as close as possible to the antiresonant condition, $T = \lambda / (4\sqrt{n^2-1})$, i.e., comparatively thicker than the struts in the photonic crystal cladding ($T \gtrsim 3S$). The combination of a thick core surround with the reduction in field intensity at the core boundary resulting from enlarging the core from 7 to 19 missing cells led to the lowest properly documented loss in a HC-PBGF to date of 1.7 dB/km at a wavelength of 1560 nm [51, 58] (Figure 5E), with mention of losses as low as 1.2 dB/km at slightly longer wavelength in a similarly structured fibre made in a further article [56]. In parallel, alternative designs incorporating antiresonant nodes in a thin core surround were also investigated and shown to provide loss improvements [59, 60] although the small 7c core employed in these works did not allow any further improvements in terms of setting a new record loss. In both cases, the thicker anti-resonant features introduced on the core boundary invariably led to an increased presence of surface modes and thus, as discussed in Section 3.3, resulted in a substantial degradation in the other key transmission properties, including decreased bandwidth and polarisation stability. As clearly shown in Figure 5, the most obvious consequence of surface modes is the effective segmentation of the low loss window into several narrower wavebands. In the case of the record-low loss fibre, the effective 3 dB transmission bandwidth is just ~20 nm [51] (see Figure 5E) – a five-fold decrease in bandwidth as compared to the earlier fibre by Corning which supported a lower number of surface modes [50] (Figure 5B). In an attempt to increase the useable transmission bandwidth and to improve the modal quality up to the demanding requirements of telecoms, large core 19c fibres were recently fabricated with a thin core surround. Despite the fact that the circular deformation of the thin boundary caused by the interplay of pressure and surface tension introduces a more substantial distortion of the first ring of holes surrounding the core, which has potential to support SMs, a 19 cell HC-PBGF with a wide (~160 nm) SM-free low loss region and a minimum transmission loss of 3.5 dB/km was demonstrated [10] (Figure 5D). The fibre provides an eight-fold bandwidth improvement as compared to the record low loss HC-PBGF (Figure 5E) [51], albeit with a factor of 2 increase in loss.

As opposed to the λ^{-4} dependence of the Rayleigh scattering in solid fibres, surface scattering loss in HC-PBGFs

designed to operate at different wavelength scales approximately as λ^{-3} [56, 57]. A λ^{-2} contribution comes from the wavelength dependence of the density of states into which scattering can occur, while the remaining λ^{-1} comes from the fact that larger rods are required in order to guide at longer wavelengths. This in turn results in the need for both a larger cladding and a larger core, the latter reducing the amount of field at the scattering air-glass interfaces. For a HC-PBGF with a given core size, however, the spectral variation of its loss within the bandgap depends more strongly on the design of the cross-sectional elements than on surface scattering, and these can therefore be engineered to increase, decrease or even substantially flatten the spectral loss profile relative to conventional fibres as the operational wavelength is increased. Note that, as discussed in more detail in Section 4.2, these fibres are few-moded and hence, as for any multimode fibre, care should be taken when measuring their loss. While modal simulations naturally provide an estimate of the loss of the various modes, the experimental determination of contributions from individual modes is more involved than in conventional single mode fibres and requires the definition of appropriate procedures. Assuming negligible or very low intermodal coupling (as is often observed in these fibres), the mode resolved loss can be measured by selectively exciting individual modes, e.g., using phase plates [61], via standard cutback. If more significant intermodal coupling were to occur in the fibre, the concept of fibre loss would become less meaningful because different modes with different loss would continuously exchange power amongst themselves, and one could at most measure the loss of the steady state combination of modes after a sufficiently long propagation distance [62].

The best documented loss levels of 1.2–1.7 dB/km (around 1550 nm) in a 19c fibre with a thick core surround is still considerably higher than theoretical simulations predict as possible. Figure 5F shows, for example, the predicted total loss (i.e., including confinement and scattering contributions) of a 37c fibre operating at 1550 nm with a hole diameter over pitch $d/\Lambda=0.99$ and an optimised rod size. Our simulations indicate that losses comparable to, or even lower, than conventional fibres might be obtained by combining progress on three different fronts: surface roughness reduction, operation at the wavelengths of minimum loss and minimisation of the electromagnetic field at the surfaces.

The smoothness of planar glass surfaces is well-known to be intrinsically limited by thermodynamics – specifically the formation of frozen-in surface capillary waves (SCWs): for more information the reader is referred to [56] and references therein. Reductions in roughness

may possibly be achieved through improved processing of the inner surfaces of HC-PBGF. The goals here are to achieve a higher surface tension and a lower glass transition temperature, both of which separately, or in combination, would lead to reduced SCW amplitudes. Other areas of future investigation that may fuel further progress in this direction also include study of the influence of strut membrane thickness on the surface roughness, the effect of glass flow on SCW formation and the study of surface roughness at spatial frequencies beyond the measurement range of AFMs, where additional roughening mechanisms quite different to those of SCWs may also exist.

Another key difference between HC-PBGFs and solid fibres is that the minimum loss wavelength for HC-PBGFs is shifted from 1.55 μm to the spectral region around 1.9–2.1 μm. Again this is due to the fact that <1% of the power of the optical mode overlaps with the glass. This considerably reduces the multi-phonon absorption loss contribution to the total fibre loss and opens up the possibility to exploit the reduction in scattering loss with increasing wavelength [56]. According to the λ^{-3} dependence of the surface scattering loss, predicted initially through dimensional analysis in [56] and more recently confirmed by numerical calculations [57], shifting the operational wavelength from 1.55 to 2 μm would reduce the minimum total fibre loss by a factor of ~2. An experimental demonstration of this was provided in [59], in which several 7c HC-PBGFs with a very similar cladding structure but different scale factors (and thus operating at different wavelength from 1400 to 2400 nm) were investigated. A minimum loss of 9.5 dB/km at 1990 nm was measured in these experiments. As will be discussed more fully in Section 5.5, this opens up intriguing possibilities for high capacity data transmission in this potentially new transmission window. The lowest loss reported for a HC-PBGF operating in this wavelength region currently stands at 4.5 dB/km in a 19c fibre similar to that shown in Figure 5E, and whose loss is shown in Figure 8B [63]. Slightly non-optimal dimension scaling and slightly increased structural distortions for this fibre relative to a comparable fibre operating at 1550 nm resulted in fairly comparable losses being measured at both wavelengths, however with fabrication improvements aimed at reducing structural deformations we can now reproduce the expected ~ factor of 2 loss reduction expected from wavelength scaling, even in 19c fibres. It is worth mentioning that another implication of the low overlap of the optical mode with the glass structure is that these fibres can guide light at wavelengths were the material absorption would be prohibitively high, opening up new prospects in, for example, mid-IR power delivery and gas sensing (see Section 5).

Finally, minimisation of the field at the interfaces can be achieved through a combination of cladding and core optimisation. The cladding can be designed such that the antiresonant operation of each rod is fully optimised, therefore contributing to the expulsion of light from the scattering surfaces. It should however be stressed that in practice the fabrication of a HC-PBGF achieving the desired cladding with optimum rod diameter, strut length and thickness is far from straightforward. The reason is that the large transverse expansion of the holey structure necessary to achieve thin struts for wide bandwidth operation forces the cladding to assume a significantly different shape in the final fibre relative to the initial preform and cane. Some preliminary work based on mass conservation principles has been recently devoted to predict such structural variations in the drawing process [11]. While more sophisticated models will be required to properly account for the very finest structural features, this model already provides useful guidance towards effective inverse designs of the optimum cane and preform required to achieve the lowest loss fibres. Additionally, the electromagnetic field at the glass surfaces can be substantially reduced further by enlarging the core radius R through omission of an increasing number of rings of holes. Since the scattering loss scales approximately as R^3 (numerical simulations in [64] show this for the fundamental mode, but the same scaling applies to all modes of the fibre), increasing the core size from 7c to 19c and from 19c to 37c would theoretically lead to a loss reduction factor of ~4.6 and ~2.7, respectively. Prompted by this consideration, we recently reported the first high air-filling fraction 37c fibre, obtaining a minimum fundamental mode loss of 3.3±0.8 dB/km at 1550 nm [55]. Whilst minor structural distortions caused significantly more scattering loss than expected from an ideal fibre, there is plenty of scope for further improvements and the result is a promising step towards further loss reduction.

4.2 Core radius, number of air-modes and modal quality

Enlarging the core is an effective way of reducing the scattering loss as we have seen above, however other modal properties of the HC-PBGF are also strongly dependent on its core radius and this need to be taken into careful consideration. For example, the number of air-guided modes increases with R^2, while the difference in effective index between the modes, proportional to how resilient the fibre is to perturbation-induced modal coupling, can be predicted to scale approximately as λ^2/R^2 – in analogy

to what happens in circular core hollow waveguides [65, 66]. Therefore, changing the size of the core defect is an effective way to realise fibres with vastly different optical properties, which can then be tailored for a specific application. Fibres with 3c, 7c, 19c and 37c have been fabricated and characterised so far, as shown in Figure 6. A summary of their optical properties is listed in Table 1, showing that a core increase corresponds to a reduction in modal power carried in the glass and in total loss, and an increase in the number of guided modes and in the mode field diameter (in the table presented as normalised to the transmission wavelength).

Historically, as it was very quickly shown theoretically that a single missing capillary would produce too small a defect to support air-guided modes [3, 21], work soon started on producing the first HC-PBGFs with a 7c core, made by omitting an additional ring of capillaries around the central one. From the very first experiments it was clear that a fibre with such a core size would support more than one (degenerate) air-guided mode [3]. In practice, with a careful launch into the Gaussian-like LP_{01} mode, and by exploiting differential modal loss over an appropriate fibre length, effectively single-mode operation with good high order mode (HOM) suppression can be achieved and this is acceptable for many applications (indeed 7c fibres have been used in most application work to date). However, for applications requiring high modal purity in short propagation lengths (for example to reduce undesired power oscillations due to modal beating in short gas cells), a strictly single mode HC-PBGF would be beneficial. With these applications in mind, a fibre with a small core based on a 3 cell core geometry was reported [8] (see Figure 6A). While as predicted from theory the scattering loss associated with a smaller core was found to be substantially higher than for a 7c version, the 3c HC-PBGF was indeed found to support only one set (comprising two orthogonal polarisations) of Gaussian-like spatial modes.

Meanwhile, another strand of research targeting low loss HC-PBGFs developed 19c and more recently 37c core fibres, which support an increasingly large number of air-guided modes. While early experimental studies immediately recognized the multimode nature of HC-PBGFs [3, 40, 45], until very recently little was known about the properties of their higher order modes. With growing interest in the applications of these fibres for data transmission and for gyroscopes, significant work has now started on understanding modality issues in HC-PBGFs. The advent of self-interferometric (S^2) imaging techniques [67] has allowed the first direct glimpse into the rich modal content supported by these fibres [68]. The S^2 measurement, typically
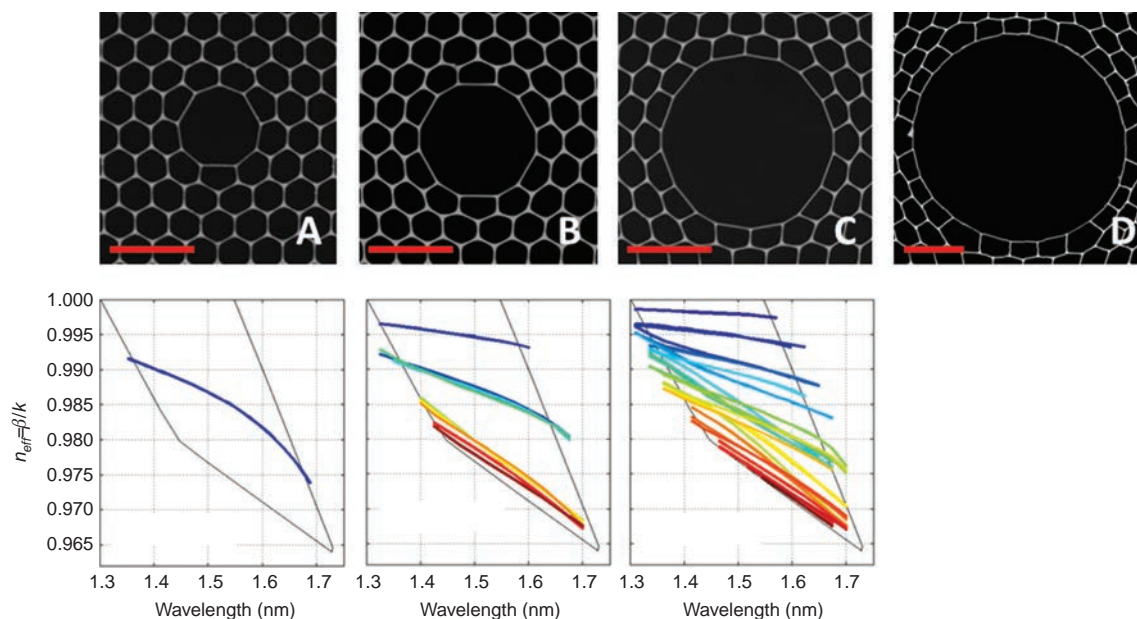
Figure 6 Investigating trade-offs between loss and modality in HC-PBGFs by varying the core size. The figure shows (top row) examples of fibres with thin core surround (and thus reduced incidence of surface modes) and increasing core element number: (A) 3 cell, showing a single mode behaviour (after [8]), (B) 7 cell, (C) 19 cell and (D) 37 cell (after [55]). For the first three fibres the corresponding simulated air-guided modes are also shown in the row below. As the core size increases, a reduction of the loss and an increase of the number of air-guided modes are theoretically predicted (see Table 1). The images are collected using a scanning electron microscope and the length bar corresponds to 10 μm.

Table 1 Summary of key properties of HC-PBGFs with increase core element number.

Property	3 cell	7 cell	19 cell	37 cell
Mode field overlap with glass	2–3%	~1%	0.2–0.4%	~0.1%
Lowest achieved loss (dB/km)	180	9.5	1.7	3.3
	[8]	[52]	[51]	[55]
Theoretical minimum loss at 2 μm (dB/km)	15	1.8	0.4	0.15
Number of air-guided vector modes	1–5	10–12	~40	~80
Mode field diameter (λ)	~2.6	~5.3	8.8–12.0	12.3–16.5

limited to short propagation lengths by the maximum detectable differential group delay (DGD), can be further combined with time-of-flight measurements [69] to gain a fuller understanding of how different modes propagate along short as well as long lengths of fibre. These measurements provide evidence of a number of well-defined air-guided modes with transverse power distributions and DGD values well matched to the theoretical predictions [65, 70]. At wavelengths sufficiently far from surface mode anti-crossings, these air-guided optical modes can be individually excited and transmitted through several hundred metres of a 19c HC-PBGF, as demonstrated for the first time in [10], see Figure 9A. The same work also showed that effectively single mode operation can be obtained through a mode selective launch and/or careful fibre splicing (see Section 5), with low levels of inter-modal distributed

cross-talk measured over lengths of at least a few hundred meters (Figure 9B).

When the core is scaled to 37c the number of modes further increases and their modal separation decreases, making 37c HC-PBGFs more susceptible to perturbation-induced intermodal coupling. Moreover, the very large MFD (see Table 1) in these fibres would suggest a higher tendency to macrobend loss. A recent experimental study however reported a 37c HC-PBGFs that, despite its large core diameter of 37 μm, demonstrated remarkable modal stability and negligible bend loss, to the point that it was used for a record data transmission capacity experiment (see Section 5) [61]. Using phase-plate-based mode multiplexing technology developed for telecoms applications, the detailed modal properties of the three lowest order modes (LP_{01}, $LP_{11a,b}$) were also investigated. Both

the fundamental and the higher order modes were found to have a wide low-loss window free of surface mode anticrossings. Due to a higher overlap with the air-glass interfaces, the $LP_{11a,b}$ modes were found to have a higher scattering loss than the LP_{01} (7.4±0.8 dB/km vs. 3.3±0.8 at 1550 nm, respectively, see Figure 10A), in agreement with modelling expectations [57].

An altogether different approach to managing the higher mode content is to actively suppress it via resonant coupling to secondary cores located in the cladding [71]. The PRISM fibre, developed by OFS Labs, contains a 19 cell central core with two 7 cell secondary cores diametrically located about it, which provide a >400 times increase in the differential loss of all higher order modes and which ensures close to strictly single mode operation despite the large core. While it should be noted that the current design only works over a narrow range of wavelengths due to the presence of residual SMs, the possibility to control the modal content irrespective of the core size is intriguing and further improvements appear both possible and likely.

5 Applications of HC-PBGFS

The unique properties of HC-PBGFs open a host of potential application opportunities, some immediately addressable, such as their use in gas sensing and gas-based nonlinear optics, but with others, such as long-haul optical communications, requiring further improvements in fibre properties and fabrication processes before they can be seriously considered. In this section we review several of the most promising/important avenues of application research, highlighting the key attractions/benefits of HC-PBGF, progress to date and future prospects. We begin this section though with consideration of a few practical issues, specifically HC-PBGF interconnection to other fibres and devices and the manufacture of in-fibre gas cells: challenges that need to be reliably solved before widespread adoption of the technology in the most interesting application areas can really take place.

The ability to obtain optically pristine fibre end-faces and low loss interconnections for HC-PBGF to both solid fibre and to itself is paramount to the successful incorporation in any practical device. As major milestones are attained in fabrication technologies and fibre development, it becomes more and more pressing to identify appropriate technological solutions to address these problems. The fibre end-faces of HC-PBGFs are known to degrade over the timescale of a few hours when exposed

to open atmosphere, and thus the ability to splice to solid fibres provides not just for stable and durable light coupling, but more importantly it also acts to prevent ingress of moisture and other undesired atmospheric gas species [4, 72]. Unfortunately the procedures established for solid fibres cannot be directly translated to HC-PBGFs. Due to their low thermal mass and large surface to volume ratio, the microstructured cladding readily deforms under excessive heat during splicing and thus the guidance properties may be significantly affected and large losses ensue if appropriate precautions are not adopted. Similarly, care has to be taken to obtain good quality fibre terminations when using cleaving tools, as the microstructure disturbs the propagation of the fracture shockwave, which can result in additional defects forming at the hole boundaries [73]. Fortunately, the latest generation of mechanical cleavers incorporating fine tension control allow the realisation of consistently good cleaves, with typical cleave angles of 0.5° or less, as required for low-loss splicing [74]. Splicing techniques to conventional fibres have been investigated for a few years now, building from the seminal work by Benabid et al. [75]. Splice losses have been reduced from 1–2 dB to the current best value of 0.42±0.09 dB [76], obtained in the case of a commercial 19c HC-PBGF spliced to a standard single mode fibre and fundamentally limited by the mode field diameter mismatch between the two fibres. The splicing strategy here relies on operating at lower fusion temperatures by reducing the time × current and offsetting the position of the arc towards the solid fibre, which results in some of the mechanical properties of the splice (and likely durability) being traded off for a lower level of structural deformation in the HC-PBGF. More recently, a different approach was demonstrated for splicing a 19c HC-PBGF to itself [74]. In this case a multi-step tack/sweep/short pulse arc was implemented on a conventional, state-of-the-art fibre splicer, which allows fusing the peripheral solid region of the fibre and results in relatively strong splices with a reported average loss of 0.16±0.05 dB. More importantly, the procedure does not appear to affect the modal properties of the fibre, with only a negligible amount of intermodal coupling measured at the splice point. The demonstration in this work that assemblies composed of multiple lengths of HC-PBGFs spliced together can allow high rate single mode data transmission with negligible power penalty provides a powerful demonstration of the effectiveness of this newly developed splicing technique.

As we shall discuss, the tight modal confinement achieved in a hollow core fibre, combined with low loss guidance, offers an excellent and practical platform to

observe and exploit gas-light interactions. The fibre geometry enables high power densities to be guided within the hollow core at relatively low input powers and over extremely long interaction lengths (10^6–10^9 times the wavelength of light), pointing to exciting opportunities both in terms of exploiting nonlinear effects in gases, and to probe weak gas-light interactions that would otherwise be difficult to observe or exploit using bulk optic approaches. Use of fibre technology also allows the fabrication of compact, fully-sealed fibre gas cells that facilitate ready experimentation and which can be directly integrated into fibre systems. The first, fully-fiberized photonic microcells (PMCs) were fabricated in 2005 [75]; a PMC is a length of gas-filled hollow core fibre which is hermetically sealed at both ends by a splice to conventional single mode fibre, which simultaneously provides low loss input and output coupling to the device. PMCs filled with both hydrogen and acetylene, for stimulated Raman scattering and laser stabilisation applications, respectively, were reported in this initial work. Following this, a more refined technique allowing the fabrication of low (vacuum) pressure PMCs was reported by Light et al. [77]. Low pressure PMCs are needed for the observation of narrow, Doppler limited or sub-Doppler gas features due to the reduced collision induced broadening they enable. Note that providing external gas access/pressure control within PMCs has also been demonstrated by micromachining holes in the side of the fibre [78, 79], see Figure 7A. Other groups have since demonstrated alternative means for the fabrication of all-fibre hollow core gas cells, for example by using specially designed fibre connectors incorporating gas inlets. These connectors keep the hollow core fibre and SMF aligned without splicing, provide low loss (<2 dB) interconnection with low Fresnel back reflection, are pressure tight and allow the gas pressure within the cell to be controlled post fabrication [80].

Finally, from a practicality perspective, it is also to be noted that HC-PBGFs are known to have low sensitivity to macrobending [81], allowing extremely small device form factors to be achieved by forming tight coils with virtually no loss penalty. This can be particularly advantageous for making very compact gas cells, gyroscopes, or for flexible high power laser delivery cabling to the micromachining work-bench. It should be noted that other waveguides providing air guidance, including hollow waveguides [82] and Kagome fibres [9] are substantially more prone to bend loss. HC-PBGFs based on smaller core defect sizes have been described as substantially immune to bend loss at wavelengths away from the bandgap edges or surface mode anti-crossings [8, 81, 83], with critical bend radii very close to, or indeed below, the fracture point of the

fibre. The bend behaviour of HC-PBGFs incorporating large core defects has also recently been investigated [61] by measuring the mode-dependent bend loss, demonstrating excellent robustness even in fibres with effective areas well in excess of 1000 μm^2. Although bend loss is a major issue with tight coils, an equally important concern is that of the mechanical reliability of the fibre under extreme stress conditions. Initial works suggest that while the mechanical strength of microstructured optical fibers can be somewhat lower than that of standard fibers, it is still adequate for many applications [84]. More research on this topic is clearly needed.

## 5.1 Nonlinear gas fibre optics

The first landmark results in nonlinear gas-based fibre optics using a HC-PBGF platform were reported by Benabid et al. in 2002 [85] who demonstrated Raman scattering threshold energies that were two orders of magnitude lower than in previous geometries by using a 1 m length of PBGF filled with hydrogen to a pressure of 17 Bar. This result kick-started the field of gas-based nonlinear fibre optics and since then a large body of work has been performed in the area, opening up access to many new in-fibre physical phenomena and many novel device opportunities. Before reviewing these we comment that whilst most of the early proof of principle work was undertaken in HC-PBGFs, the focus in more recent years has been progressively moved towards the use of another class of hollow core fibre, the so-called anti-resonant fibre (ARF), which guides in air due to antiresonances associated with a thin array of glass struts located about a hollow core. This includes fibres with a Kagome cladding arrangement [9] as well as fibres with a simplified cladding made of just one ring of air holes around the core and either a hexagram shape [86] or a negative curvature core boundary [87, 88]. Although the minimum absolute loss achievable in ARFs is considerably higher (by orders of magnitude) than that of HC-PBGF, in many applications the typical device lengths are just a few metres or less, and propagation loss is therefore not an issue. ARFs appear to provide more desirable dispersive properties (lower slopes and absolute dispersion values) than HC-PBGFs, broader bandwidths and larger cores. Moreover, their dispersive and nonlinear characteristics can be readily tuned through appropriate choice of gas type and pressure. It is to be noted however that ARFs are substantially more prone to bend loss than HC-PBGFs and this is an important practical consideration if compact devices are required. For the purpose of this review we will only discuss work involving HC-PBGFs.

For more information on ARFs and their applications we refer the readers to [9].

Through appropriate fibre design it is possible to engineer gas-filled HC-PBGFs with well-defined anomalous dispersion and controllable Kerr and Raman nonlinearity such that optical soliton effects previously demonstrated in solid fibres in the near IR can be exploited at wavelengths down into the UV [89] or at far greater than MW peak power levels (around 1000× higher than in solid fibres) [90]. For example, by appropriate choice of gas it is possible to control the relative strength of the Kerr and Raman nonlinearities (e.g., by selecting mono-atomic gases such as Argon, Raman effects can be effectively eliminated so as to provide a pure Kerr fibre medium, alternatively one can use a mixture of cases of differing Raman responses to generate a tailored Raman gain profile). Using carefully engineered nonlinear/dispersive gas-filled HC-PBGFs the following exemplar device applications have been demonstrated: pulse compression down to pulses of a few cycles duration [89]; efficient dispersive wave generation at wavelengths in the UV [89] (e.g., allowing conversion efficiencies of ~15% from a pump source operating around 800 nm down to <200 nm); High Harmonic Generation (HHG) at reduced pulse energies [91] (~100 nJ rather than the ~1 mJ usually required in free space embodiments); and finally access to light-plasma interactions in fibres [92]. For a relatively recent review on ultrafast nonlinear gas-filled fibre optics the interested reader is referred to [93]. Note that in addition to research that exploits ultrafast Kerr effects in gases, use of other resonant nonlinear effects in gases and alkali-metal vapours is also possible and significant results have been demonstrated in fields including electromagnetically induced transparency [94], saturated absorption spectroscopy [95], microwave plasma generation [96] and optical switching at the few photon level [97].

5.2 Gas sensing and frequency reference cells

The first spectroscopy measurements in HC-PBGFs date back to 2004 when experiments on acetylene were reported using a simple intensity-based measurement approach [98]. Numerous papers on the use of similar and more advanced spectroscopy techniques (e.g., correlation spectroscopy [99], saturated absorption spectroscopy [95]) on an increasingly diverse range of gases (including ammonia [100], methane [101] (see Figure 7B) and carbon-dioxide [102]) are to be found in the literature with reasonably
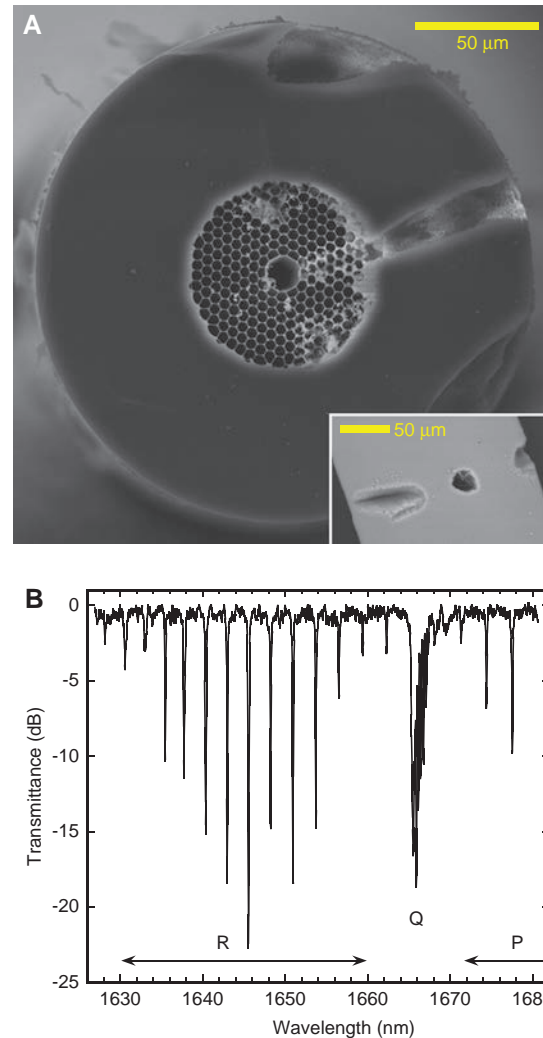
Figure 7 Gas sensing using HC-PBGFs. (A) Access side-channels fabricated via femtosecond laser micromachining. The channels connect the hollow core directly to the outside environment and provide for a much faster in-diffusion of gaseous species leading to a reduced sensor response time [78] (B) Detection of methane gas (CH_4) at ~1.6 µm using a HC-PBGF [101].

impressive sensitivities claimed (e.g., 10 parts per million by volume achieved for methane). Most measurements to date have used the first overtone absorption lines in the near IR. However, with the realisation of silica-based HC-PBGFs operating with losses well below 1 dB/m and very wide transmission bandwidths in the mid-IR extending out to 3.8 µm and possibly beyond (see Figure 8A) [103], the opportunity to make reliable measurements on the much stronger fundamental absorption peaks exists [104] and should help further increase the sensitivities and specificities achievable. One clear issue for any hollow core fibre (HCF) approach is the time taken for gases to diffuse into and out of the fibre, which limits the measurement speeds
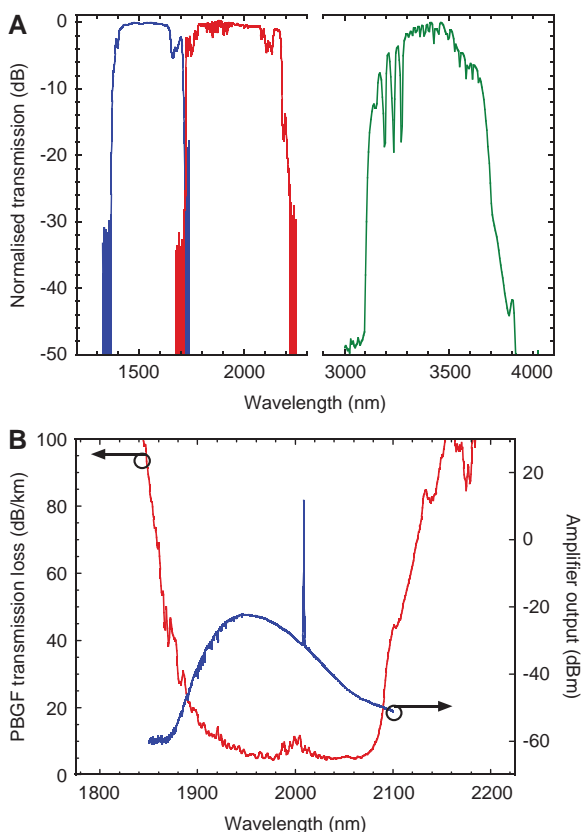
Figure 8 Long wavelength transmission in HC-PBGFs. (A) Normalised transmission of ~5 m lengths of HC-PBGFs illustrating the possibility of scaling the operating wavelength of these fibres much deeper in the mid-IR than is possible using conventional silica fibres [103]. (B) Low loss, wide bandwidth HC-PBGF designed for operation in the predicted region of minimum loss around 2 μm. Also shown is the output of a Thulium-doped amplifier with amplified data channel. The extent of the amplified stimulated emission (in blue) illustrates the gain bandwidth of the Thulium amplifier and the excellent match with the transmission bandwidth of the HC-PBGF [63].

possible. Drilling gas-access holes into the fibre along its length (see Figure 7A) [78] can improve the response time but this comes with an associated potential risk of compromising the optical and mechanical integrity of the fibre over time. Maximising the core size whilst ensuring suitable modal quality for the given measurement technique is thus also important. For completeness, it should also be mentioned that as well as allowing gas sensing it is also possible to develop a range of sensors that use the controlled ingression of liquids into the cladding/core holes and exploit the different guidance mechanism possible in microstructured fibres (i.e., index guiding and photonic band gap depending on the index differences between the liquid and the silica/air microstructure) (see e.g., [105]). Moreover, laser-based macroscopic particle guidance is

also possible through HC-PBGFs as first demonstrated in [106] and of relevance to applications in fundamental science and fields such as biology and medicine, amongst others.

The use of PMCs for gas reference cells represents an extremely attractive and natural application of HC-PBGFs, and considerable work in this direction has by now been reported. The initial demonstration focused on the use of acetylene-filled cells for laser locking applications around 1550 nm as needed for various telecommunications/test and measurement or metrology applications [75]. However, as previously discussed, progressively, more sophisticated techniques have subsequently been developed in order to fill cells with a broader range of gases and vapour types at the pressures required to achieve the spectral linewidths/cell absorptions per-unit-length needed for different uses. Tests proving the reliability and durability of cells over many years have also now been undertaken (at least for certain gas types). With environmental and pollution monitoring an ever increasing issue, the development of compact gas reference cells appears an important technology. Again, the benefits of HC-PBGFs relative to ARFs in gas sensing are likely to accrue in applications where long path lengths/compact gas cells are needed due to the lower losses and reduced bend sensitivities that they offer, although, since they typically possess a smaller core diameter, wall-collision induced line broadening/depolarisation effects occurs more rapidly and gases take longer to diffuse along the fibre length.

5.3 Laser beam delivery

HC-PBGFs offer significant advantages over conventional solid fibre technology when it comes to the delivery of high power laser radiation. Firstly, the relative overlap of the mode with solid region of the fibre is low (typically <1% in most HC-PBGF designs of relevance, see Table 1) and since the nonlinearity of air and of most gases is less than a thousandth that of silica, the nonlinearity per-unit-length of HC-PBGF is typically a thousandth or so, of that of a solid fibre of equivalent core size. Secondly, the intensities at the air/glass interface of a HC-PBGF are substantially lower than those at the centre of the core of a solid fibre of similar core size at equal power delivery levels. Consequently, HC-PBGFs can in principle handle far more optical power before catastrophic damage and/or optical nonlinearities cut in and limit performance. While this can be beneficial in the CW regime, e.g., in applications in which the delivery of narrow linewidth radiation is required (which is prone to limitations due to Stimulated Brillouin Scattering

(SBS)) the primary benefits arise in the delivery of pulsed laser light. These are needed in diverse uses ranging from industrial materials processing, through to important applications in biology and medicine such as multi-photon microscopy and the treatment of various skin conditions. The improved performance of HC-PBGFs relative to solid fibres has been proven in experiments demonstrating the delivery of nanosecond pulse at ~mJ pulse energies (over greater distances than possible in solid fibres) [107], as well as in experiments in both the ps [108] and fs regimes [109, 110]. ARFs also compete with HC-PBGFs in these applications, with HC-PBGFs providing advantages with regard to loss and bend loss (a particularly important feature for laser beam delivery) and with ARFs offering benefits in terms of the delivery of shorter pulses due to the inherently lower and flatter dispersion over broad bandwidths and the increased core sizes possible. Note however that in some instances the dispersion of the HC-PBGF can be used to good effect in the delivery of laser light: for example to compress linearly chirped pulses directly from an oscillator [111], within an external amplifier system [112], or as a compressor in Chirped Pulse Amplification (CPA) in which the pulse is stretched by a significant factor (e.g., ×1000) prior to amplification and re-compressed thereafter in order to avoid optical nonlinearities within the amplifier [113]). Nonlinear pulse compression can also be exploited in HC-PBGs at far higher pulse energies than in solid fibres due to the far lower nonlinearities possible: either using soliton effects [114], or using self-phase modulation (SPM) and a final stage of pulse compression using bulk gratings, prisms or chirped mirrors [115]. As well as being used for the external delivery of fibre laser radiation it is also worth noting that HC-PBGFs have been used to provide low-nonlinearity intracavity dispersion compensation within femtosecond fibre lasers [116]. One of the attractions here is that they can provide normal or anomalous dispersion at wavelengths where this is not possible using conventional solid single mode fibres (e.g., anomalous dispersion at wavelengths below 1200 nm). Note that recent progress on extending low loss transmission to the mid-IR in HCFs also promises new capabilities in the delivery of mid-IR radiation [103]. This is likely to have most impact in the field of medicine, allowing for example the delivery of radiation at 2.94 μm as used in many surgical procedures due to the strong water absorption at this wavelength [117].

5.4 Optical fibre sensing

We have previously discussed HC-PBGFs in the context of absorption-based gas sensing; however they have other attributes that make them interesting for other sensing applications besides. For a relatively recent review of this topic see [118]. Firstly, by virtue of their construction, they are less susceptible to thermally-induced index changes [119] and can in principle be fabricated to be more sensitive to strain and external pressure [120]. The reduced thermal sensitivity offers potential environmental stability benefits in interferometric sensing e.g., for pressure, strain and acoustic field measurement applications. Indeed a number of interferometric sensors based on HC-PBGFs spliced to SMFs with flat cleaved end-facets to define Fabry-Perot interferometers have been reported [121] which have allowed direct verification of the reduced temperature sensitivity. Polarimeters based on HC-PBGFs have also been shown [122].

One of the most successful of all fibre sensors is the fibre gyroscope based on the Sagnac interferometer and HC-PBGFs are generating interest here also. Critical to this application, as well as a low thermal sensitivity, is the low-Rayleigh backscattering and low optical nonlinearity since these effects can otherwise serve to compromise system resolution. Excellent single mode, polarisation maintaining (or in some implementations polarising) performance of the fibre are further essential requirements. HC-PBGFs offer potential benefits on all of these fronts and as a consequence various groups are looking to realise these benefits in practice [123]. Recent work on large core HC-PBGFs with effectively single mode behaviour based on resonant stripping of higher-order modes looks particularly promising for these applications [71].

Several sensor applications, particularly those associated with space borne missions or with use in nuclear plant/waste management, require long-term operation of fibres in high radiation environments. Again HC-PBGFs offer potential advantages: both in terms of use in the sensor elements themselves, but also in terms of signal transmission to and from sensors. Conventional fibres tend to darken when exposed to radiation, and while this can be reduced to some extent and radiation-hardened fibres produced, these still degrade with time. By contrast HC-PBGFs are relatively resilient to the effects of radiation since the signal is propagating primarily in air/vacuum, with just a small proportion of the signal in the solid glass regions of the fibre prone to radiation damage [124, 125].

5.5 Optical communications

The optical communications systems of today are based on the use of conventional solid-core silica fibres which, as a result of more than 40 years of continuous refinement

and huge research investment, are manufactured in high volume with propagation losses as low as 0.149 dB/km, thus close to the theoretical minimum imposed by Rayleigh scattering of the core glass. This represents a staggering engineering achievement. Equally remarkable, as a result of sustained technological developments and key advances such as the invention of the erbium doped fibre amplifier (EDFA), the development of Wavelength Division Multiplexing (WDM) and more recently the development of digital coherent transmission, we are close to realising the ultimate practical information carrying transmission capability (~100 TBit/s) of conventional fibres in the laboratory. This capacity limit is imposed by the optical nonlinearity/loss of standard transmission fibres and there is little room left for optimisation of the existing technology [126]. Since their very first demonstration, the possibility that HC-PBGFs might ultimately offer lower losses than solid core fibres was recognised. It was also widely appreciated that the reduced nonlinearity would also aid data transmission and that the reduced group velocity would allow for low latency transmission. However, it rapidly became apparent that achieving low loss in HC-PBGFs would be immensely challenging and that the presence of other supported modes (both higher-order core guided modes and surface modes) were likely to compromise the prospects of realising a low loss, high capacity waveguide. The low nonlinearity and low latency were however assured by virtue of the basic guidance mechanism. As a consequence, despite very substantial programs on HC-PBGF loss reduction within various companies and university groups up until the mid-2000s, only very limited data transmission experiments were ever reported at that time.

The only real data transmission experiment using a HC-PBGF prior to recent times was reported by Peucheret et al. in 2005 [127] who demonstrated the transmission of a single 10 Gbits/s data stream over a total HC-PBGF length of 150 m. However, even over this distance and at this relatively low data rate, significant transmission penalties were observed, likely due to the unsuppressed presence of surface modes at wavelengths nearby. Given that the HC-PBGF loss reduction work ground to a halt soon after these experiments and the fact that these transmission results were relatively disappointing, no further research in this direction was reported for several years.

However, due to improvements in the understanding of the guidance properties, advances in the design and fabrication of such fibres and the emerging realisation that existing solid fibre technology is close to its capacity limits, interest has again turned to considering HC-PBGFs for data transmission – both in terms of achieving high
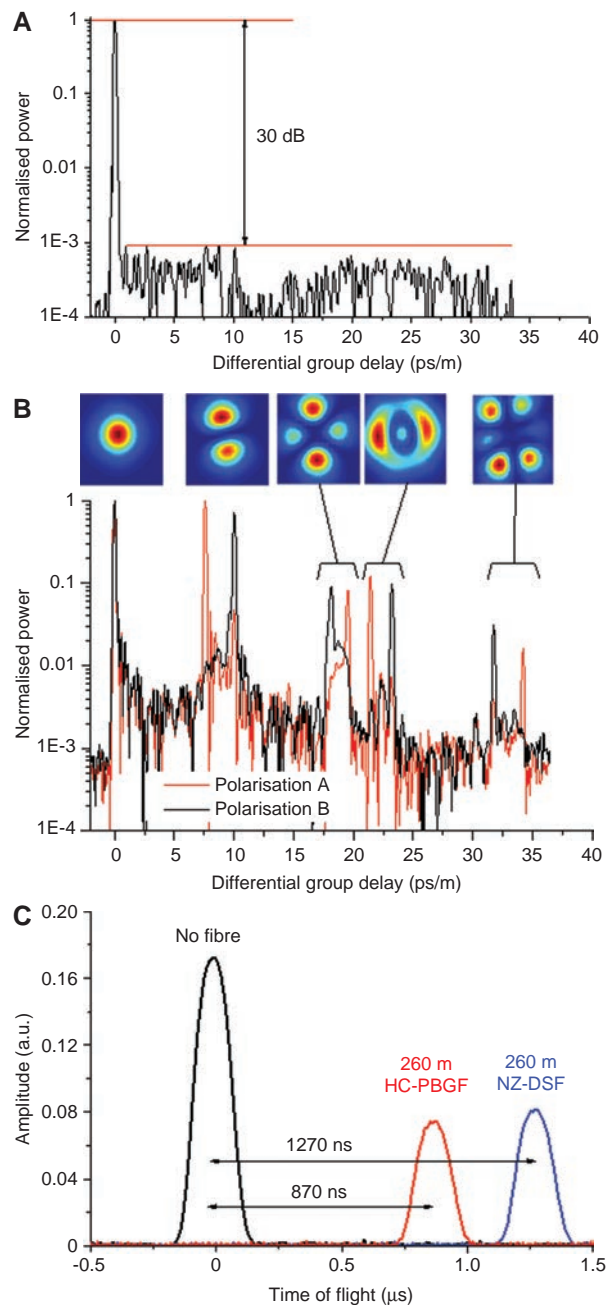
Figure 9 Characterisation of modal and latency properties of HC-PBGFs using time-of-flight measurements obtained by transmitting a ~1 ps pulsed laser though 240 m length of low loss, wide bandwidth 19c HC-PBGF. Due to a smaller group velocity, higher order modes are detected at progressively longer delays from the fundamental mode. (A) shows that by optimizing the coupling and polarization at launch and by using a single mode solid fibre at the output as a spatial filter the fundamental mode can be transmitted with as high as~30 dB suppression of higher order modes [10]; (B) an unoptimised offset launch shows a rich high order mode content, which can be further selected by using polarisation control [10]; (C) time-resolved measurements through the same length of hollow and solid fibre, showing that in HC-PBGFs optical signals travel close to the speed of light in vacuum, i.e., ~30% faster than in conventional fibres [10].

capacities but also now in terms of exploiting the low latency aspects directly, irrespective of their other interesting potential attributes. Advances in the use of Digital Signal Processing of coherent optical signals to eliminate cross-talk/modal interference through the Multiple Input Multiple Output (MIMO) concept (which raises the possibility of using each guided mode as the basis of an independent data channel, [128]) is also of high relevance given the multimode nature of candidate designs for low loss HC-PBGFs. Substantial work restarted on investigating HC-PBGFs for data transmission in 2011 [64, 126].

A landmark result was the realisation of a 19c HC-PBGF with a bandwidth significantly wider than the current C+L bands of telecommunications (160 nm) and a loss sufficiently low (3.5 dB/km, see fibre D of Figure 5) to be of interest for data transmission [10]. By taking care to excite and detect just the fundamental mode at the input and output of the fibre and to operate at wavelengths far from surface mode anticrossings, effectively single mode operation with relatively low levels of inter-modal distributed cross-talk was demonstrated over fibre lengths of a few 100 m (see Figure 9B), and more recently ~1 km [74]. A sufficiently low level of intermodal cross-talk to allow the use of high spectral efficient modulation formats (including both 16 and 32 QAM coding) was demonstrated. This allowed data transmission at record aggregate capacities of order 30 Tbit/s (96 wavelength channels across the C-Band and 20 GBaud, 32QAM coding) over ~250 m of 19c HC-PBGF [129].

Absolute time of flight measurements (ToF) in the same fibre confirmed the added benefit of a ~31% reduction in signal latency with signal propagation at 99.7% the speed of light in vacuum, see Figure 9C [10]. Wide bandwidth signal transmission with low-latency is emerging as a key requirement in a number of important application areas. For example, reducing the data transmission latency across computer networks has become critical in improving the performances of modern massively parallelised supercomputers, which tend to be bottlenecked by their slowest sequential process and which is often associated with the distribution of data. Likewise, a similar desire for reduced latency data transmission comes from financial institutions, prepared to invest large fortunes for the competitive advantage to be gained from receiving data before their competitors. Many large scale scientific experiments, for example in high energy physics environments, also require vacuum light speed for control/synchronisation and optimum data taking. The first experiments confirming successful, low-latency data transmission in HC-PBGFs have recently been reported [10]. Whilst the current minimum losses are still too high

to permit long-haul, low latency transmission the current losses are still more than adequate for many of the aforementioned applications, resulting in considerable interest in the technology.

Further ToF experiments in the same 19c fibre used in the 1550 nm low latency experiments but this time using an offset launch at the input provided a clear demonstration that different optical modes guided in the fibre can be individually excited and transmitted (see Figure 9A). These results confirmed the possibility of exploiting Mode-Division Multiplexing (MDM) in these fibres as a means to increase the per-fibre capacity. Significant progress has now been made in this direction, from a first demonstration of MDM in a HC-PBGF [130] to the current record transmission capacity in these fibres, see Figure 10, [55]. To date, transmission on two mode groups (LP_{01} and LP_{11} – corresponding to 6 modes in total allowing for all degeneracies and polarisations) has been achieved with MIMO processing used to eliminate the effects of mode coupling within the system. These experiments have so far been performed at 1550 nm and still over relatively modest length scales in terms of long haul systems (~350 m). However total capacities in excess of 73 Tbit/s have been demonstrated [55] in a 37c HC-PBGF, and considerable scope to extend this substantially further in terms of number of modes and transmission distance exists. The critical issues that still need to be addressed to allow further progress relate to control of differential mode group delays (DMGDs) and Differential Modal Loss (DML), along with management of the inherent mode-coupling along the fibre length itself. These effects ultimately define the level of computational complexity of the MIMO DSP required and hence the practicality of the approach.

All of the HC-PBGF transmission results described previously were performed at the conventional transmission waveband of 1550 nm, however as discussed in Section 4 the minimum loss transmission window in HC-PBGFs is likely to occur at wavelengths around 2000 nm. In order to ultimately support long distance transmission in these fibres, an optical amplifier operational in this waveband is thus required. Fortunately there is a candidate amplification system based on thulium doped fibres (see Figure 8B) that appears capable of providing very similar performance to the EDFA at 1550 nm [131], moreover with the benefits of a considerably larger optical bandwidth. The first transmission experiments at 2000 nm in HC-PBGF incorporating thulium doped fibre amplifiers (TDFAs) have indeed now been reported [63]. Furthermore, the development of the various critical optical devices (e.g., transmitters, receivers, filters etc.) needed to enable high capacity WDM
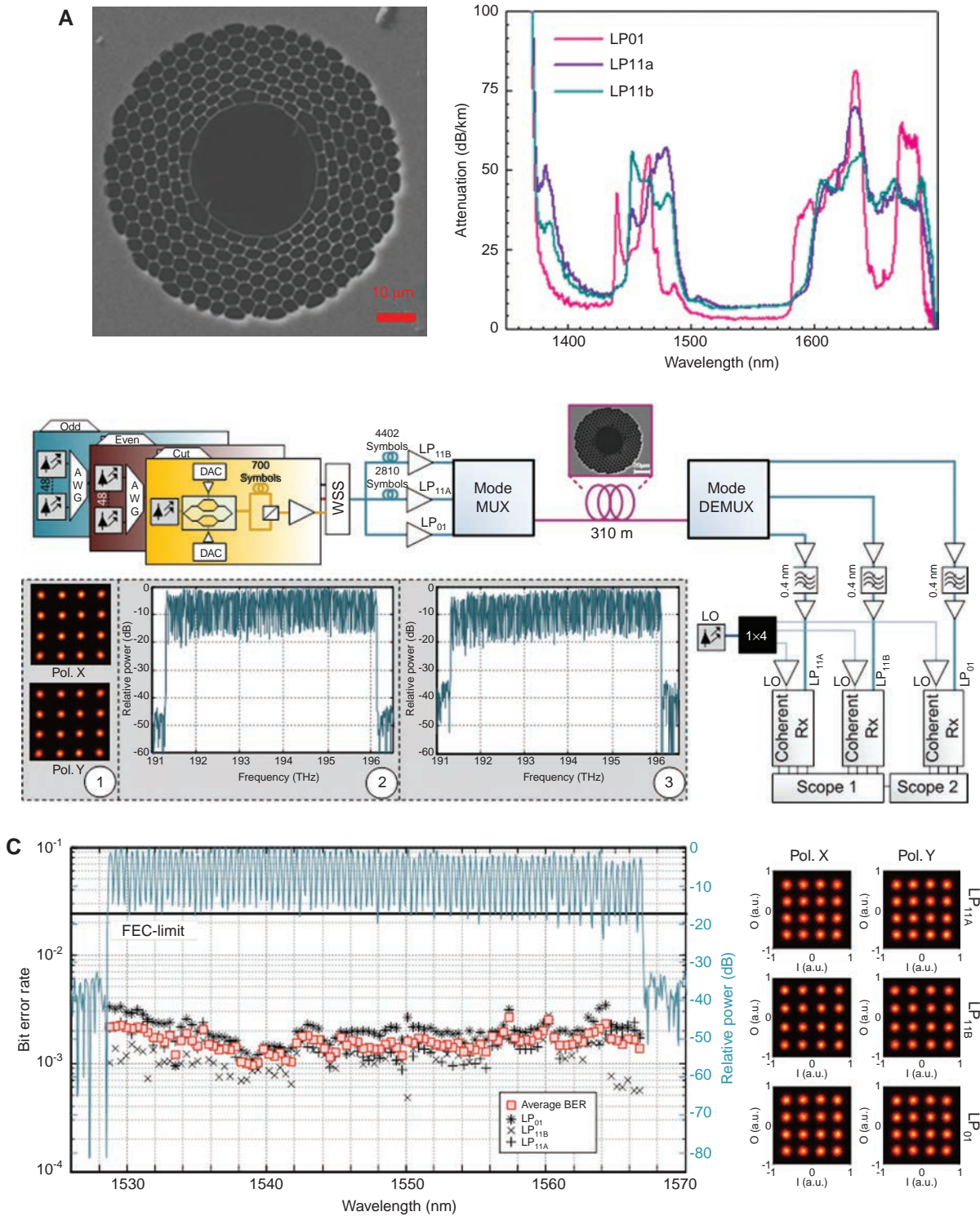
Figure 10 (A) SEM of the 37c fiber used for high capacity MIMO-based MDM transmission along with a modally resolved loss measurement showing increasing loss with increasing mode order. (B) Experimental set up for MDM transmission with inset showing both the WDM channel allocation and input 16 PDM:QAM constellation diagram. (C) Transmission results showing successful 96 WDM channel, 6-mode (3×MDM×2PDM), 25 GBaud/s 16 QAM transmission over 350 m of HC-PBGF [55].

transmission is also well underway and the first WDM experiments have also now been undertaken [132]. If the predicted ultralow loss of HC-PBGFs can be realized, then all of the key components required to build high capacity communication links at this emerging waveband are now in place.

6 Conclusions

In conclusion, we have provided an overview of the current status of the field of HC-PBGFs, describing the latest understanding of the fundamental guidance mechanism and issues limiting the current/ultimate performance of this relatively new class of optical fibres. We have also described the current status of HC-PBGF fabrication, reporting some of the most recent achievements in driving the propagation loss down whilst maximizing the usable bandwidth and ensuring the well-conditioned modal characteristics needed for many of the most interesting and lucrative applications. Finally, we have briefly reviewed some of the most interesting device/systems uses of the technology, discussing in particular progress towards using HC-PBGFs as data transmission media for both long and short haul communications where they offer some unique benefits relative to conventional (solid) fibre technology.

As can be seen, enormous advance has been made on all aspects of HC-PBGF technology since the first demonstration in 1999. Real world applications in laser power delivery and in devices based on light:gas interactions already appear within sight, as arguably are certain specialist short haul communications usages, such as within data centres and supercomputers where latency is key and the distances involved are relatively modest. However, it is apparent that significant further research will be required if they are ever to realise their full potential in long haul telecommunications applications, where far longer lengths of fibre are needed and the cost and reliability are so onerous. Further work on loss reduction and means for reliable volume manufacture are critical in the short term and major programs are again now looking at these key issues – only time will tell where this will ultimately lead but much interesting fundamental science and engineering will be done along the way and benefits will accrue in all other application areas along the way.

References

[1] Tonucci RJ, Justus BL, Campillo AJ, Ford CE. Nanochannel array glass. Science 1992;258:783–5.

[2] Knight JC, Birks TA, Russell PS, Atkin DM. All-silica single-mode optical fiber with photonic crystal cladding. Opt Lett 1996;21:1547–9.

[3] Cregan RF, Mangan BJ, Knight JC, Birks TA, Russell PS, Roberts PJ, Allan DC. Single-mode photonic band gap guidance of light in air. Science 1999;285:1537–9.

[4] Gretlund JS, Jakobsen C, Lyngso JK, Simonsen HR. US Patent No. US20100266251 A1. 2010.

[5] Chen Y, Birks TA. Predicting hole sizes after fibre drawing without knowing the viscosity. Opt Mat Express 2013;3:346–56.

[6] Petrovich MN, Amezcua-Correa R, Broderick NGR, Richardson DJ, Delmonte T, Watson MA, O'Driscoll EJ. Photonic bandgap fibres for broadband transmission of SWIR wavelengths. Presented at the Electro Magnetic Remote Sensing (EMRS) Defense Technology Centre (DTC) conference 2006, paper B19.

[7] Amezcua-Correa R, Petrovich MN, Broderick NG, Richardson D. Broadband Infrared Transmission in a Hollow-Core Photonic Bandgap Fibre Free of Surface Modes. Presented at the European Conference on Optical Communications (ECOC) 2006, paper We4.4.4.

[8] Petrovich MN, Poletti F, van Brakel A, Richardson DJ. Robustly single mode hollow core photonic bandgap fiber. Opt Express 2008;16:4337–46.

[9] Benabid F, Roberts PJ. Linear and nonlinear optical properties of hollow core photonic crystal fiber. J Mod Optic 2011;58:87–124.

[10] Poletti F, Wheeler NV, Petrovich MN, Baddela N, Fokoua EN, Hayes JR, Gray DR, Li Z, Slavík R, Richardson DJ. Towards high-capacity fibre-optic communications at the speed of light in vacuum. Nat Photonics 2013;7:279–84.

[11] Fokoua EN, Petrovich MN, Baddela NK, Wheeler NV, Hayes JR, Poletti F, Richardson DJ. Real-time prediction of structural and optical properties of hollow-core photonic bandgap fibers during fabrication. Opt Lett 2013;38:1382–4.

[12] Bise RT, Trevor DJ. Sol-gel Derived Microstructured Fibers: Fabrication and Characterization. Presented at the Optical Fiber Communication Conference (OFC) 2005, paper OWL6.

[13] Webb A, Poletti F, Richardson DJ, Sahu J. Suspended-core holey fibre for evanescent-field sensing. Optical Engineering Letters 2007;46:p.010503.

[14] Becker M, Werner M, Fitzau O, Esserb D, Kobelkea J, Lorenza A, Schwuchowa A, Rothhardta M, Schustera K, Hoffmannb D, Bartelta H. Laser-drilled free-form silica fiber preforms for microstructured optical fibers. Opt Fiber Technol 2013;19:482–5.

[15] Joannopoulos JD, Johnson SG, Winn JN, Meade RD. Photonic crystals: molding the flow of light. 2nd ed. Princeton: Princeton University Press; 2008.

[16] Russell PSJ, Birks TA, Lloyd-Lucas FD. Photonic bloch waves and photonic band gaps. Presented at the Confined Electrons and Photons: New Physics and Applications 1995.

[17] Russell PSJ. Photonic-crystal fibers. J Lightwave Technol 2006;24:4729–49.

[18] Birks TA, Roberts PJ, Russell PSJ, Atkin DM, Shepherd TJ. Full 2-D photonic bandgaps in silica/air structures. Electron Lett 1995;31:1941–3.

[19] Birks TA, Bird DM, Hedley TD, Pottage JM, Russell PSJ. Scaling laws and vector effects in bandgap-guiding fibres. Opt Express 2004;12:69–74.

[20] Barkou SE, Broeng J, Bjarklev A. Silica-air photonic crystal fiber design that permits waveguiding by a true photonic bandgap effect. Opt Lett 1999;24:46–8.

[21] Broeng J, Barkou SE, Sondergaard T, Bjarklev A. Analysis of air-guiding photonic bandgap fibers. Opt Lett 2000;25:96–8.

[22] Mortensen NA, Nielsen MD. Modeling of realistic cladding structures for air-core photonic bandgap fibers. Opt Lett 2004;29:349–51.

[23] Maradudin AA, McGurn AR. Out-of-plane propagation of electromagnetic-waves in a 2-dimensional periodic dielectric medium. J Mod Optic 1994;41:275–84.

[24] Meade RD, Brommer KD, Rappe AM, Joannopoulos JD. Existence of a photonic band-gap in 2 Dimensions. Appl Phys Lett 1992;61:495–7.

[25] West JA, Fajardo J, Gallagher M, Koch K, Borrelli N, Allan D. Demonstration of an IR-optimized air-core photonic band-gap fiber. Presented at the European Conference on Optical Communication (ECOC) 2000, paper Th.A.2.

[26] Saitoh K, Koshiba M. Leakage loss and group velocity dispersion in air-core photonic bandgap fibers. Opt Express 2003;11:3100–9.

[27] White TP, McPhedran RC, Botten LC, Smith GH, de Sterke CM. Calculations of air-guided modes in photonic crystal fibers using the multipole method. Opt Express 2001;9:721–32.

[28] Aghaie KZ, Fan SH, Digonnet MJF. Birefringence Analysis of photonic-bandgap fibers using the hexagonal yee's cell. IEEE J Quantum Elect 2010;46:920–30.

[29] Birks TA, Pearce GJ, Bird DM. Approximate band structure calculation for photonic bandgap fibres. Opt Express 2006;14:9483–90.

[30] Poletti F, Richardson DJ. Hollow-core photonic bandgap fibers based on a square lattice cladding. Opt Lett 2007;32:2282–4.

[31] Yan M, Shum P. Air guiding with honeycomb photonic bandgap fiber. IEEE Photonic Tech L 2005;17:64–66.

[32] Poletti F. Hollow core fiber with an octave spanning bandgap. Opt Lett 2010;35:2837–9.

[33] Dong LA, Thomas BK, Suzuki S, Fu LB. Extending transmission bandwidth of air-core photonic bandgap fibers. Opt Fiber Technol 2010;16:442–8.

[34] Light PS, Couny F, Wang YY, Wheeler NV, Roberts PJ, Benabid F. Double photonic bandgap hollow-core photonic crystal fiber. Opt Express 2009;17:16238–43.

[35] Pottage JM, Bird DM, Hedley TD, Birks TA, Knight JC, St. Russell PJ, Roberts PJ. Robust photonic band gaps for hollow core guidance in PCF made from high index glass. Opt Express 2003;11:2854–61.

[36] Hu J, Menyuk CR. Leakage loss and bandgap analysis in air-core photonic bandgap fiber for nonsilica glasses. Opt Express 2007;15:339–49.

[37] Desevedavy F, Renversez G, Troles J, Houizot P, Brilland L, Vasilief I, Coulombier Q, Traynor N, Smektala F, Adam J-L. Chalcogenide glass hollow core photonic crystal fibers. Opt Mater 2010;32:1532–9.

[38] Allan DC, Borrelli NF, Gallagher MT, Müller D, Smith CM, Venkataraman N, West JA, Zhang P, Koch KW. Surface modes and loss in air-core photonic band-gap fibers. Presented at the Photonic Crystal Materials and Devices 2003, SPIE Proceedings, vol. 5000, pp 161–74.

[39] Saitoh K, Mortensen NA, Koshiba M. Air-core photonic band-gap fibers: the impact of surface modes. Opt Express 2004;12:394–400.

[40] Humbert G, Knight JC, Bouwmans G, St. Russell J, Williams DP, Roberts PJ, Mangan BJ. Hollow core photonic crystal fibers for beam delivery. Opt Express 2004;12:1477–84.

[41] Poletti F, Broderick NGR, Richardson DJ, Monro TM. The effect of core asymmetries on the polarization properties of hollow core photonic band gap fibers. Opt Express 2005;13:9115–24.

[42] Wegmuller M, Legre M, Gisin N, Hansen TP, Jacobsen C, Broeng J. Experimental investigation of the polarization properties of a hollw core photonic bandgap fiber for 1550 nm. Opt Express 2005;13:1457–67.

[43] Digonnet MJF, Kim HK, Shin J, Fan S, Kino GS. Simple geometric criterion to predict the existence of surface modes in air-core photonic-bandgap fibers. Opt Express 2004;12:1864–72.

[44] Kim HK, Digonnet MJF, Kino GS, Shin J, Fan S. Simulations of the effect of the core ring on surface and air-core modes in photonic bandgap fibers. Opt Express 2004;12:3436–42.

[45] West JA, Smith CM, Borrelli NF, Allan DC, Koch KW. Surface modes in air-core photonic band-gap fibers. Opt Express 2004;12:1485–96.

[46] Amezcua-Correa R, Broderick NG, Petrovich MN, Poletti F, Richardson DJ. Design of 7 and 19 cells core air-guiding photonic crystal fibers for low-loss, wide bandwidth and dispersion controlled operation. Opt Express 2007;15:17577–86.

[47] Amezcua-Correa R, Broderick NGR, Petrovich MN, Poletti F, Richardson DJ. Optimizing the usable bandwidth and loss through core design in realistic hollow-core photonic bandgap fibers. Opt Express 2006;14:7974–85.

[48] Poletti F, Numkam Fokoua E.Understanding the Physical Origin of Surface Modes and Practical Rules for their Suppression. Presented at the ECOC 2013, paper Tu.3.A.4.

[49] Couny F, Benabid F, Roberts PJ, Burnett MT, Maier SA. Identification of Bloch-modes in hollow-core photonic crystal fiber cladding. Opt Express 2007;15:325–38.

[50] Smith CM, Venkataraman N, Gallagher MT, Müller D, West JA, Borrelli NF, Allan DC, Koch KW. Low-loss hollow-core silica/air photonic bandgap fibre. Nature 2003;424:657–9.

[51] Mangan BJ, Farr L, Langford A, Roberts PJ. Low loss (1.7 dB/km) hollow core photonic bandgap fiber. Presented at the Optical Fiber Communication Conference (OFC) 2004, paper PD24.

[52] Amezcua-Correa R, Gerome F, Leon-Saval SG, Broderick NGR, Birks TA, Knight JC. Control of surface modes in low loss hollow-core photonic bandgap fibers. Opt Express 2008;16:1142–9.

[53] West JA, Venkataramam N, Smith CM, Gallagher MT. Photonic crystal fibers. Presented at the European Conference on Optical Communications (ECOC) 2001, paper Th.A.2.2.

[54] Lyngsø JK, Jakobsen C, Simonsen HR, Broeng J. Single-mode 7-cell core hollow core photonic crystal fiber with increased bandwidth. Presented at the International Conference on Optical Fiber Sensors 2011, Proc. SPIE 7753, 21st International Conference on Optical Fiber Sensors, 77533Q (2011).

[55] Sleiffer V, Jung Y, Baddela N, Surof J. High capacity mode-division multiplexed optical transmission in a novel 37-cell hollow-core photonic bandgap fiber. J Lightwave Technol 2013;PP:1–1. http://dx.doi.org/10.1109/JLT.2013.2274194.

[56] Roberts PJ, Couny F, Sabert H, Mangan BJ, Williams DP, Farr L, Mason MW, Tomlinson A, Birks TA, Knight JC, St. Russell PJ. Ultimate low loss of hollow-core photonic crystal fibres. Opt Express 2005;13:236–44.

[57] Fokoua EN, Poletti F, Richardson DJ. Analysis of light scattering from surface roughness in hollow-core photonic bandgap fibers. Opt Express 2012;20:20980–91.

[58] Roberts PJ, Williams DP, Mangan BJ, Sabert H, Couny F, Wadsworth WJ, Birks TA, Knight JC, St. Russell PJ. Realizing low loss air core photonic crystal fibers by exploiting an antiresonant core surround. Opt Express 2005;13:8277–85.

[59] Lyngsø JK, Mangan BJ, Jakobsen C, Roberts PJ. 7-cell core hollow-core photonic crystal fibers with low loss in the spectral region around 2 mu m. Opt Express 2009;17:23468–73.

[60] Roberts PJ, Williams DP, Sabert H, Mangan BJ, Bird DM, Birks TA, Knight JC, St. Russell PJ. Design of low-loss and highly birefringent hollow-core photonic crystal fiber. Opt Express 2006;14:7329–41.

[61] Jung Y, Sleiffer VAJM, Baddela NK, Petrovich M, Hayes JR, Wheeler N, Gray D, Fokoua ERN, Wooler J, Wong N, Parmigiani F, Alam S-U, Surof J, Kuschnerov M, Veljanovski V, de Waardt H, Poletti F, Richardson DJ. First demonstration of a broadband 37-cell hollow core photonic bandgap fiber and its application to high capacity mode division multiplexing. Presented at the Optical Fiber Communication Conference (OFC) 2013, paper PDP5A.3.

[62] Marcuse D. Theory of dielectric optical waveguides. 2nd ed. San Diego, CA: Academic Press; 1991.

[63] Petrovich MN, Poletti F, Wooler J, Heidt A, Baddela NK, Li Z, Gray DR, Slavík R, Parmigiani F, Wheeler N, Hayes J, Fokoua EN, Grüner-Nielsen L, Pálsdóttir B, Phelan R, Kelly B, Becker M, MacSuibhne N, Zhao J, Gunning FCG, Ellis A, Petropoulos P, Alam S-U, Richardson D. First Demonstration of 2µm Data Transmission in a Low-Loss Hollow Core Photonic Bandgap Fiber. Presented at the European Conference and Exhibition on Optical Communication (ECOC) 2012, paper Th.3.A.5.

[64] Morioka T, Awaji Y, Ryf R, Winzer P, Richardson D, Poletti F. Enhancing optical communications with brand new fibers. IEEE Communications Magazine 2012;50:S31–42.

[65] Poletti F, Numkam Fokoua E, Petrovich MN, Wheeler NV, Baddela NK, Hayes JR, Richardson D. Hollow Core Photonic Bandgap fibers for Telecommunications: Opportunities and Potential Issues. Presented at the Optical Fiber Communication Conference (OFC) 2012, paper OTh1H.3.

[66] Marcatili EA, Schmeltzer RA. Hollow core and dielectric waveguides for long distance optical transmission and lasers. Bell Syst Tech J 1964;43:1783–809.

[67] Nicholson JW, Yablon AD, Fini JM, Mermelstein MD. Measuring the modal content of large-mode-area fibers. IEEE J Sel Top Quant 2009;15:61–70.

[68] Nicholson JW, Meng L, Fini JM, Windeler RS, DeSantolo A, Monberg E, DiMarcello F, Dulashko Y, Hassan M, Ortiz R. Measuring higher-order modes in a low-loss, hollow-core, photonic-bandgap fiber. Opt Express 2012;20:20494–505.

[69] Gray DR, Li Z, Poletti F, Slavík R, Wheeler N, Baddela NK, Petrovich MN, Obeysekara A, Richardson D. Complementary Analysis of Modal Content and Properties in a 19-cell Hollow Core Photonic Band Gap Fiber using Time-of-Flight and S2 Techniques. Presented at the European Conference and Exhibition on Optical Communication (ECOC) 2012, paper Mo.2.F.1.

[70] Digonnet MJF, Kim HK, Kino GS, Fan SH. Understanding air-core photonic-bandgap fibers: Analogy to conventional fibers. J Lightwave Technol 2005;23:4169–77.

[71] Fini JM, Nicholson JW, Windeler RS, Monberg EM, Meng L, Mangan B, DeSantolo A, DiMarcello FV. Low-loss hollow-core fibers with improved single-modedness. Opt Express 2013;21:6233–42.

[72] Wheeler NV, Petrovich MN, Baddela NK, Hayes JR, Fokoua EN, Poletti F, Richardson DJ. Gas Absorption between 1.8 and 2.1 µm in Low Loss (5.2 dB/km) HC-PBGF. Presented at the Conference on Lasers and Electro-Optics (CLEO) 2012, paper CM3N.5.

[73] Francois V, Aboutorabi SS. A mechanical criterion for the design of readily cleavable microstructured optical fibers. Opt Express 2006;14:7312–8.

[74] Wooler J, Gray D, Poletti F, Petrovich M, Wheeler N, Parmigiani F, Richardson DJ. Robust Low Loss Splicing of Hollow Core Photonic Bandgap Fiber to Itself. Presented at the Optical Fiber Communication Conference (OFC) 2013, paper OM3I.5.

[75] Benabid F, Couny F, Knight JC, Birks TA, Russell PS. Compact, stable and efficient all-fibre gas cells using hollow-core photonic crystal fibres. Nature 2005;434:488–91.

[76] Thapa R, Knabe K, Corwin KL, Washburn BR. Arc fusion splicing of hollow-core photonic bandgap fibers for gas-filled fiber cells. Opt Express 2006;14:9576–83.

[77] Light PS, Couny F, Benabid F. Low optical insertion-loss and vacuum-pressure all-fiber acetylene cell based on hollow-core photonic crystal fiber. Opt Lett 2006;31:2538–40.

[78] van Brakel A, Grivas C, Petrovich MN, Richardson DJ. Micro-channels machined in microstructured optical fibers by femtosecond laser. Opt Express 2007;15:8731–6.

[79] Hensley CJ, Broaddus DH, Schaffer CB, Gaeta AL. Photonic band-gap fiber gas cell fabricated using femtosecond microma-chining. Opt Express 2007;15:6690–5.

[80] Marty PT, Morel J, Feurer T. All-fiber multi-purpose gas cells and their applications in spectroscopy. J Lightwave Technol 2010;28:1236–40.

[81] Hansen TP, Broeng J, Jakobsen C, Vienne G, Simonsen HR, Nielsen MD, Skovgaard PMW, Folkenberg JR, Bjarklev A. Air-guiding photonic bandgap fibers: spectral properties, macrobending loss, and practical handling. J Lightwave Technol 2004;22:11–5.

[82] Harrington JA. A review of IR transmitting, hollow waveguides. Fiber Integrated Opt 2000;19:211–27.

[83] Shephard JD, MacPherson WN, Maier RRJ, Jones J, Hand D, Mohebbi M, George A, Roberts P, Knight J. Single-mode mid-IR guidance in a hollow-core photonic crystal fiber. Opt Express 2005;13:7139–44.

[84] Sonnenfeld C, Sulejmani S, Geernaert T, Eve S, Gomina M, Makara M, Skorupski K, Mergo P, Berghmans F, Thienpont H. Mechanical reliability of microstructured optical fibers: a comparative study of tensile and bending strength. Presented at the Microstructured and Specialty Optical Fibres Conference 2012, Proc. SPIE 84260Q; doi: 10.1117/12.923184.

[85] Benabid F, Knight JC, Antonopoulos G, Russell PSJ. Stimulated Raman scattering in hydrogen-filled hollow-core photonic crystal fiber. Science 2002;298:399–402.

[86] Poletti F, Hayes JR, Richardson DJ.Optimising the performances of hollow antiresonant fibres. Presented at the European Conference on Optical Communication (ECOC) 2011, paper Mo.2.LeCervin.2.

[87] Pryamikov AD, Biriukov AS, Kosolapov AF, Plotnichenko VG, Semjonov SL, Dianov EM. Demonstration of a waveguide regime for a silica hollow – core microstructured optical fiber with a negative curvature of the core boundary in the spectral region >3.5 mu m. Opt Express 2011;19:1441–8.

[88] Yu F, Knight JC. Spectral attenuation limits of silica hollow core negative curvature fiber. Opt Express 2013;21:21466–71.

[89] Joly NY, Nold J, Chang W, Hölzer P, Nazarkin A, Wong GKL, Biancalana F, St. Russell PJ. Bright spatially coherent wavelength-tunable deep-UV laser source using an ar-filled photonic crystal fiber. Phys Rev Lett 2011;106:203901.

[90] Ouzounov DG, Ahmad FR, Muller D, Venkataraman N, Gallagher MT, Thomas MG, Silcox J, Koch KW, Gaeta AL. Generation of megawatt optical solitons in hollow-core photonic band-gap fibers. Science 2003;301:1702–4.

[91] Heckl OH, Baer CRE, Krankel C, Marchese SV, Schapper F, Holler M, Sudmeyer T, Robinson JS, Tisch JWG, Couny F, Light P. High harmonic generation in a gas-filled hollow-core photonic crystal fiber. Appl Phys B-Lasers O 2009;97:369–73.

[92] Holzer P, Chang W, Travers JC, Nazarkin A, Nold J, Joly NY, Saleh MF, Biancalana F, Russell PS. Femtosecond nonlinear fiber optics in the ionization regime. Phys Rev Lett 2011;107:203901.

[93] Travers JC, Chang WK, Nold J, Joly NY, Russell PSJ. Ultrafast nonlinear optics in gas-filled hollow-core photonic crystal fibers [Invited]. J Opt Soc Am B 2011;28:A11–26.

[94] Ghosh S, Sharping JE, Ouzounov DG, Gaeta AL. Resonant optical interactions with molecules confined in photonic band-gap fibers. Phys Rev Lett 2005;94:093902.

[95] Couny F, Light PS, Benabid F, Russell PS. Electromagnetically induced transparency and saturable absorption in all-fiber devices based on (C2H2)-C-12-filled hollow-core photonic crystal fiber. Opt Commun 2006;263:28–31.

[96] Debord B, Gérôme F, Jamier R, Boisse-Laporte C, Leprince P, Leroy O, Blondy J-M, Benabid F. First Ignition of an UV Microwave Microplasma in Ar-filled Hollow-Core Photonic Crystal Fibers. Presented at the European Conference and Exposition on Optical Communications (ECOC) 2011, paper Mo.2.LeCervin.5.

[97] Venkataraman V, Saha K, Gaeta AL. Phase modulation at the few-photon level for weak-nonlinearity-based quantum computing. Nat Photonics 2013;7:138–41.

[98] Ritari T, Tuominen J, Ludvigsen H, Petersen JC, Sørensen T, Hansen TP, Simonsen HR. Gas sensing using air-guiding photonic bandgap fibers. Opt Express 2004;12:4080–7.

[99] Austin E, van Brakel A, Petrovich MN, Richardson DJ. Fibre optical sensor for C2H2 gas using gas-filled photonic bandgap fibre reference cell. Sensor Actuat B-Chem 2009;139:30–4.

[100] Cubillas AM, Hald J, Petersen JC. High resolution spectroscopy of ammonia in a hollow-core fiber. Opt Express 2008;16:3976–85.

[101] Cubillas AM, Lazaro JM, Conde OM, Petrovich MN, Lopez-Higuera JM. Gas sensor based on photonic crystal fibres in the 2 nu(3) and nu(2)+2 nu(3) vibrational bands of methane. Sensors-Basel 2009;9:6261–72.

[102] Nwaboh JA, Hald J, Lyngso JK, Petersen JC, Werhahn O. Measurements of CO2 in a multipass cell and in a hollow-core photonic bandgap fiber at 2 mu m. Appl Phys B-Lasers O 2013;110:187–94.

[103] Wheeler N, Heidt AM, Baddela N, Hayes JR, Sandoghchi SR, Fokoua EN, Poletti F, Petrovich MN, Richardson DJ. Low Loss, Wide Bandwidth, Low Bend Sensitivity HC-PBGF for Mid-IR Applications. Presented at the Workshop on Specialty Optical Fiber and Their Applications (WSOF) 2013.

[104] Gayraud N, Kornaszewski LW, Stone JM, Knight JC, Reid DT, Hand DP, MacPherson WN. Mid-infrared gas sensing using a photonic bandgap fiber. Appl Optics 2008;47:1269–77.

[105] Fini JM. Microstructure fibres for optical sensing in gases and liquids. Meas Sci Technol 2004;15:1120–8.

[106] Benabid F, Knight JC, Russell PS. Particle levitation and guidance in hollow-core photonic crystal fiber. Opt Express 2002;10:1195–203.

[107] Shephard JD, Couny F, Russell PS, Jones JDC, Knight JC, Hand DP. Improved hollow-core photonic crystal fiber design for delivery of nanosecond pulses in laser micromachining applications. Appl Optics 2005;44:4582–8.

[108] Konorov SO, Fedotov AB, Kolevatova OA, Beloglazov VI, Skibina NB, Shcherbakov AV, Wintner E, Zheltikov AM. Laser breakdown with millijoule trains of picosecond pulses transmitted through a hollow-core photonic-crystal fibre. J Phys D-Appl Phys 2003;36:1375–81.

[109] Peng XA, Mielke M, Booth T. High average power, high energy 1.55 mu m ultra-short pulse laser beam delivery using large mode area hollow core photonic band-gap fiber. Opt Express 2011;19:923–32.

[110] Lanin AA, Fedotov IV, Sidorov-Biryukov DA, Doronina-Amitonova LV, Ivashkina OI, Zots MA, Sun C-K, Ömer Ilday F, Fedotov AB, Anokhin KV, Zheltikov AM. Air-guided photonic-crystal-fiber pulse-compression delivery of multimegawatt femtosecond laser output for nonlinear-optical imaging and neurosurgery. Appl Phys Lett 2012;100:101104.

[111] Nielsen CK, Jespersen KG, Keiding SR. A 158 fs 5.3 nJ fiber-laser system at 1 mu m using photonic bandgap fibers for dispersion control and pulse compression. Opt Express 2006;14:6063–8.

[112] Gerome F, Dupriez P, Clowes J, Knight JC, Wadsworth WJ. High power tunable femtosecond soliton source using hollow-core photonic bandgap fiber, and its use for frequency doubling. Opt Express 2008;16:2381–6.

[113] De Matos CJS, Taylor JR, Hansen TP, Hansen KP, Broeng J. All-fiber chirped pulse amplification using highly-dispersive air-core photonic bandgap fiber. Opt Express 2003;11:2832–7.

[114] Welch MG, Cook K, Correa RA, Gérôme F, Wadsworth WJ, Gorbach AV, Skryabin DV, Knight JC. Solitons in hollow core photonic crystal fiber: engineering nonlinearity and compressing pulses. J Lightwave Technol 2009;27:1644–52.

[115] Rothhardt J, Hädrich S, Carstens H, Herrick N, Demmler S, Limpert J, Tünnermann A. 1 MHz repetition rate hollow fiber pulse compression to sub-100-fs duration at 100 W average power. Opt Lett 2011;36:4605–7.

[116] Lim H, Wise FW. Control of dispersion in a femtosecond ytterbium laser by use of hollow-core photonic bandgap fiber. Opt Express 2004;12:2231–5.

[117] Urich A, Maier RRJ, Mangan BJ, Renshaw S, Knight JC, Hand DP, Shephard JD. Delivery of high energy Er:YAG pulsed laser light at 2.94 mu m through a silica hollow core photonic crystal fibre. Opt Express 2012;20:6677–84.

[118] Jin W, Xuan HF, Ho HL. Sensing with hollow-core photonic bandgap fibers. Meas Sci Technol 2010;21:094014.

[119] Dangui V, Kim HK, Digonnet MJF, Kino GS. Phase sensitivity to temperature of the fundamental mode in air-guiding photonic-bandgap fibers. Opt Express 2005;13:6669–84.

[120] Pang M, Jin W. Detection of acoustic pressure with hollow-core photonic bandgap fiber. Opt Express 2009;17:11088–97.

[121] Rao YJ, Deng M, Zhu T, Li H. In-line fabry-perot etalons based on hollow-corephotonic bandgap fibers for high-temperature applications. J Lightwave Technol 2009;27:4360–5.

[122] Xuan HF, Jin W, Zhang M, Ju J, Liao YB. In-fiber polarimeters based on hollow-core photonic bandgap fibers. Opt Express 2009;17:13246–54.

[123] Digonnet M, Blin S, Kim HK, Dangui V, Kino G. Sensitivity and stability of an air-core fibre-optic gyroscope. Meas Sci Technol 2007;18:3089–97.

[124] Girard S, Baggio J, Leray JL. Radiation-induced effects in a new class of optical waveguides: the air-guiding photonic crystal fibers. IEEE T Nucl Sci 2005;52:2683–8.

[125] Olanterä L, Sigaud C, Troska J, Soos C, Vasey F, Petrovich MN,Wooler J, Wheeler N, Poletti F, Richardson DJ. Gamma Irradiation of Hollow-Core Photonic Bandgap Fibres. Presented at the Topical Workshop in Electronics for Particle Physics (TWEPP) 2013. http://indico.cern.ch/internalPage. py?pageId=2&confId=228972.

[126] Desurvire E, Kazmierski C, Lelarge F, Marcadet X, Scavennec A, Kish FA, Welch DF, Nagarajan R, Joyner CH, Schneider RP, Corzine SW, Kato M, Evans PW, Ziari M, Dentai AG, Pleumeekers JL, Muthiah R, Bigo S, Nakazawa M, Richardson DJ, Poletti F, Petrovich MN, Alam SU, Loh WH, Payne DN. Science and technology challenges in XXIst century optical communications. C R Phys 2011;12:387–416.

[127] Peucheret C, Zsigri B, Hansen TP, Jeppesen P. 10 Gbit/s transmission over air-guiding photonic bandgap fibre at 1550 nm. Electron Lett 2005;41:27–29.

[128] Randel S, Ryf R, Sierra A, Winzer PJ, Gnauck AH, Bolle CA, Essiambre RJ, Peckham DW, McCurdy A, Lingle R. 6x56-Gb/s mode-division multiplexed transmission over 33-km few-mode fiber enabled by 6x6 MIMO equalization. Opt Express 2011;19:16697–707.

[129] Sleiffer VAJM, Jung Y, Leoni P, Kuschnerov M, Wheeler NV, Baddela N, van Uden RGH, Okonkwo CM, Hayes JR, Wooler J, Numkam E, Slavik R, Poletti F, Petrovich MN, Veljanovski V, Alam SU, Richardson DJ, de Waardt H. 30.7 Tb/s (96x320 Gb/s) DP-32QAM transmission over 19-cell Photonic Band Gap Fiber. Presented at the Optical Fiber Communication Conference (OFC) 2013, paper OW1I.5.

[130] Xu J, Peucheret C, Lyngso JK, Leick L. Two-mode multiplexing at 2 x 10.7 Gbps over a 7-cell hollow-core photonic bandgap fiber. Opt Express 2012;20:12449–56.

[131] Li Z, Heidt AM, Daniel JMO, Jung Y, Alam SU, Richardson DJ. Thulium-doped fiber amplifier for optical communications at 2 mu m. Opt Express 2013;21:9289–97.

[132] Mac Suibhne N, Li Z, Baeuerle B, Zhao J, Wooler J, Alam S-U, Poletti F, Petrovich M, Heidt A, Wheeler N, Baddela N, Fokoua ERN, Giles I, Giles D, Phelan R, O'Carroll J, Kelly B, Corbett B, Murphy D, Ellis AD, Richardson DJ, Gunning FG. WDM Transmission at 2μm over Low-Loss Hollow Core Photonic Bandgap Fiber. Presented at the Optical Fiber Communication Conference (OFC) 2013, paper OW1I.6.